Chapter 10

TCHINHADZANDZE GRANODIORITE GNEISS

10.1 Introduction

The Tchinhadzandze Granodiorite Gneiss occurs within an area occupied by the Early Proterozoic Messica Granite Gneiss and the Frontier Formation. The distinctive characteristic of this granite is that it does not show the strong planar fabrics which characterize the eastern exposures of the Messica Granite Gneiss and therefore it is either late- or post-tectonic with respect to that deformation.

10.2 Field Description

This gneiss occurs as bodies generally associated with the metasediments of the Frontier Formation and their better exposures are at Tchinhadzandze (Fig. 2.2). The granite is grey and contains feldspar which predominates over quartz, biotite and hornblende and locally exhibits feldspar phenocrysts. The rock is weakly foliated, and the foliation is, defined by biotite and hornblende randomly oriented. It is weakly jointed and cut by thin quartz-feldspar and pegmatitic veins.

10.3 Petrography

The granite is inequigranular, medium grained (Fig. 10.1), and locally exhibits preferred orientation of biotite and hornblende. The feldspars exhibit perthitic and myrmeckitic intergrowths.
The mineralogy is dominated by plagioclase and includes quartz, K-feldspar, hornblende and biotite. Minor phases are titanite, epidote and zircon (Table 10.1).

Table 10.1: Mineralogical assemblage (proportions of each mineral indicated) of Tchinhadzandze Granodiorite Gneiss.

sample	K-fld	Plg	Qtz	Bt	Hbl	Ep	Ttn
ygr1	24	42	25	4	4	<1	1
ygr2	23	45	22	4	5	-	1
ygr3	22	45	24	3	5	<1	1
ygr4	23	43	23	5	6	<1	-
ygr5	23	42	25	4	5	-	1
ygr6	22	44	24	5	5	<1	-

K-fld- potassium feldspar, Plg- plagioclase, Qtz- quartz, Bt- biotite, Hbl- Hornblende, Ep- epidote and Ttn- titanite.

K-Feldspar occurs as anhedral grains exhibiting cross-hatched (mostly) and Carlsbad twins whereas plagioclase exhibits albite and Carlsbad twinning. Both feldspar types are cracked and contain inclusions of finer quartz and feldspar grains.

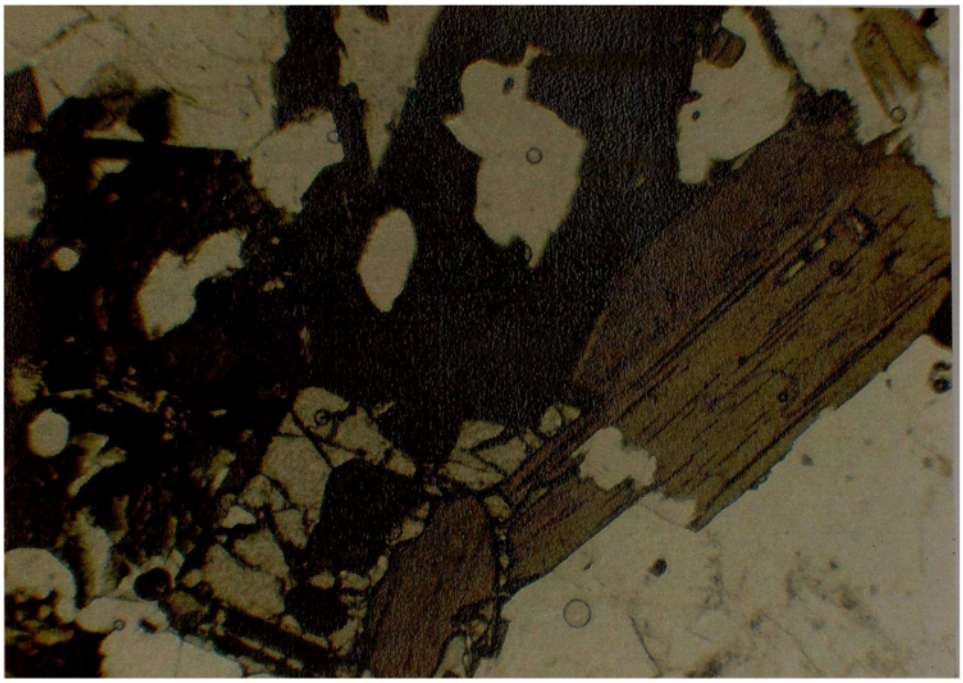

Figure 10.1: Inequigranular medium grained granite gneiss. Minerals shown are feldspar (white), green hornblende containing inclusions of feldspar and quartz, brown biotite and dark grey titanite (high relief) associated with hornblende and biotite. Parallel light, width of field 7 mm.

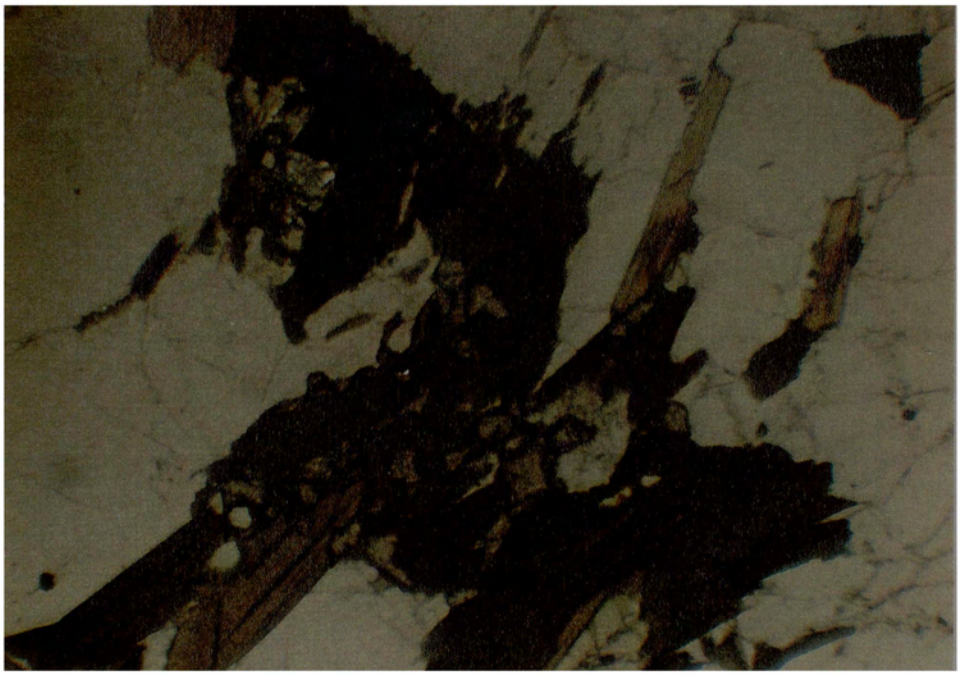

Figure 10.2: Preferred orientation of biotite and hornblende. Note fine-grained titanite (high relief) associated with the hornblende and biotite. Parallel light, width of field 7 mm.

Anhedral quartz contains inclusions of feldspar and shows undulatory extinction indicating that the granite has been strained. Brown biotite forms subhedral grains which locally show preferred orientation. Green hornblende grains, commonly associated with biotite, are subhedral to anhedral and contain inclusions of feldspar, quartz and titanite. (Fig. 10.2). Titanite occurs as fine to medium grains associated with ferromagnesian minerals either along grain boundaries or as inclusions (Fig. 10.2). Epidote occurs as an alteration product of amphibole and plagioclase. Zircon is rare and occurs as prismatic fine grains.

10.4 Chemistry

10.4.1 Introduction

The samples were analysed for major and trace element compositions (Table 10.2) and two of them were analysed for REE (Table 10.3).

10.4.2 Major Element Chemistry

The major element compositions of the samples show little variation. Total iron and MgO contents result in ΣFeO/MgO ratios of ~3:1.

Table 10.2: Major and trace elements analyses of samples from Tchinhadzandze Granodiorite Gneiss.

Sample	YGR1	YGR2	YGR3	YGR4	YGR5	YGR6
SiO_2	70.48	69.17	68.21	69.37	69.51	69.9
$Al_{i2}O_3$	14.7	15.23	15.24	15.13	15.04	14.87
Fe_2O_3	1.19	1.44	1.50	1.25	1.39	1.31
FeO	1.42	1.82	1.90	1.58	1.72	1.60
MgO	1.16	1.36	1.43	1.34	1.33	1.36
CaO	2.28	2.64	2.85	2.5	2.55	2.46
Na_2O	4.02	4.05	3.93	3.91	3.76	4.02
K_2O	4.24	3.82	3.9	3.94	4.26	4.13
TiO_2	0.37	0.41	0.4	0.37	0.4	0.39
P_2O_5	0.14	0.18	0.19	0.17	0.2	0.18
MnO	0.03	0.06	0.05	0.04	0.05	0.05
total	**100.03**	**100.18**	**99.60**	**99.60**	**100.21**	**100.27**
Ba	1612	1351	1548	1539	1634	1550
Co	36	37	36	38	36	43
Cr	33	36	37	33	34	35
Cu	15	5	5	4	7	8
Li	15	16	15	17	15	14
Nb	4	4	5	5	4	4
Ni	18	22	24	25	22	21
Sc	3	5	5	6	6	5
Sr	618	576	620	614	592	616
Rb	86	93	92	88	94	87
V	29	39	40	32	35	36
Y	8	11	11	10	12	12
Zn	162	53	52	47	51	51
Zr	128	182	167	147	213	219
Ga	17	19	20	18	20	19

The Na_2O+CaO contents are ~6 wt% with K_2O ~4 wt% which results in the samples plotting on the boundaries between the granodiorite, adamellite trondhjemite and granite fields in terms of normative albite, orthoclase and anorthite on the Barker (1979) diagram (Figure 10.3). According to Shand's alumina saturation Index the rocks are metaluminous (Fig. 10.4). Although the range of SiO_2 values is small, Harker variation diagrams show linear trends of decreasing Al_2O_3, Fe_2O_3, MgO, FeO and CaO contents with increasing SiO_2 whereas Na_2O and K_2O increase with SiO_2 (Figs. 10.5, 10.6 and 10.7). Low MgO and ΣFeO relative to Σalkalis result in the granite being calc-alkaline in nature (Fig. 10.8).

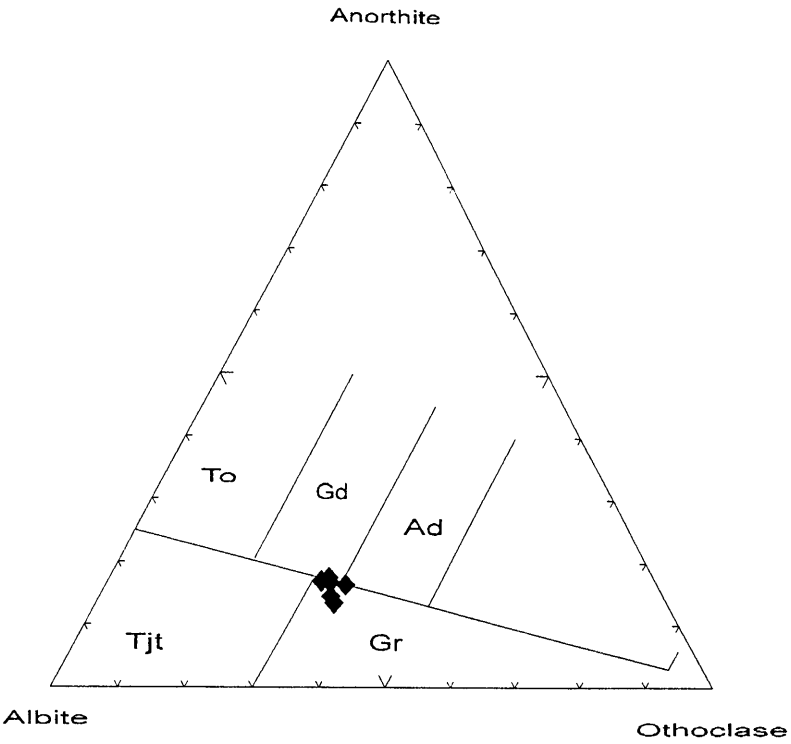

Figure 10.3: Plot of Tchinhadzandze Granodiorite Gneiss in the normative albite, orthoclase and anorthite diagram (after Barker, 1979). The boundary between trondhjemites (Tjt) and granite (Gr) and the boundary between these two fields and the fields of tonalites (To), granodiorite (Gd) and adamellites (Ad) are from O'Connor (1965).

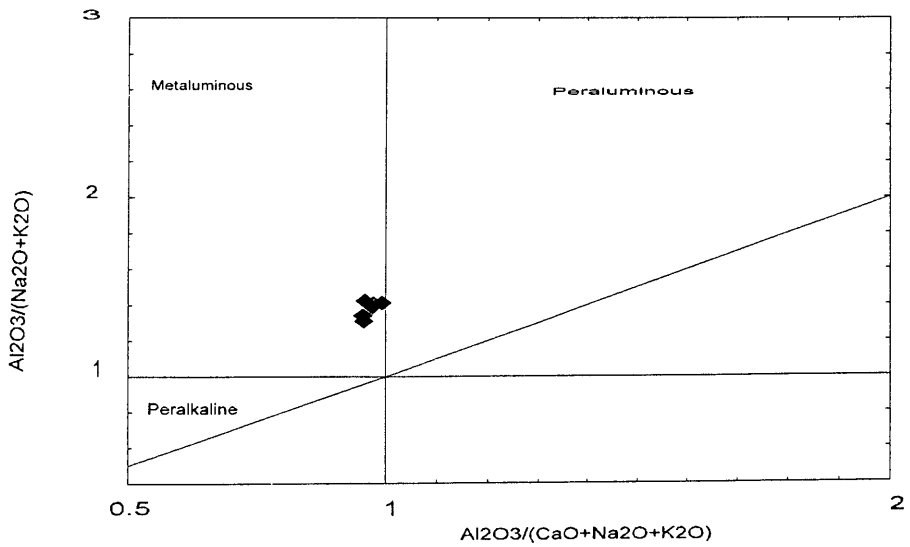

Figure 10.4: Shands 's (1947) alumina saturation Index diagram plotting samples of the Tchinhadzandze Granodiorite Gneiss as metaluminous.

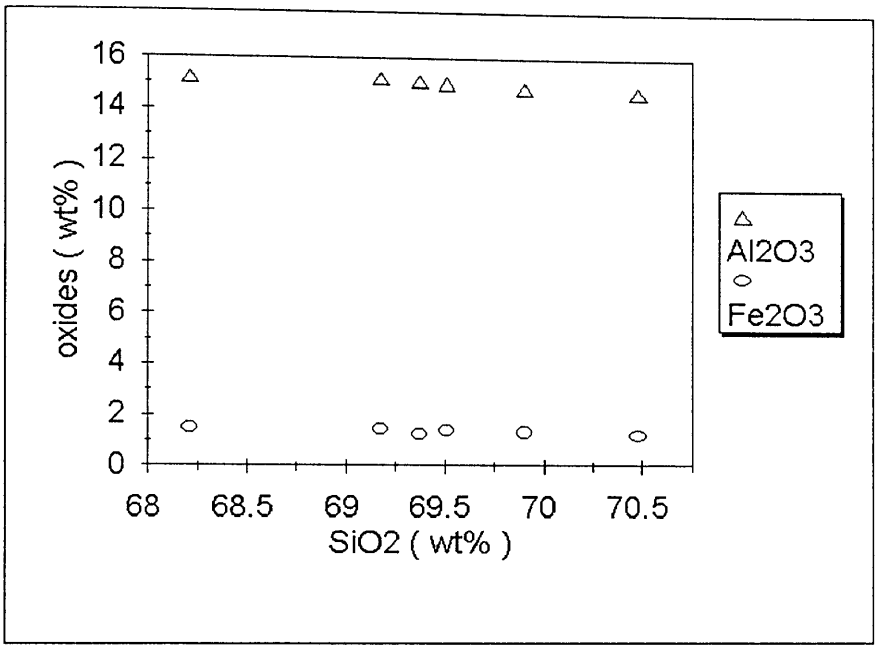

Figure 10.5: Al_2O_3 and Fe_2O_3 versus SiO$_2$ variation diagram of Tchinhadzandze Granodiorite Gneiss.

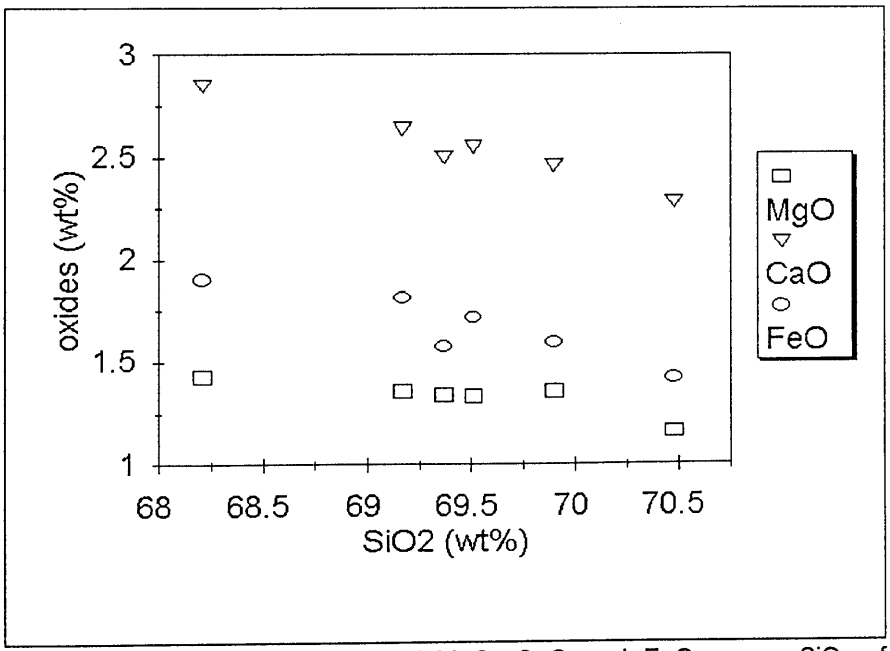

Figure 10.6: Variation diagram of MgO, CaO and FeO versus SiO_2 of Tchinhadzandze Granodiorite Gneiss.

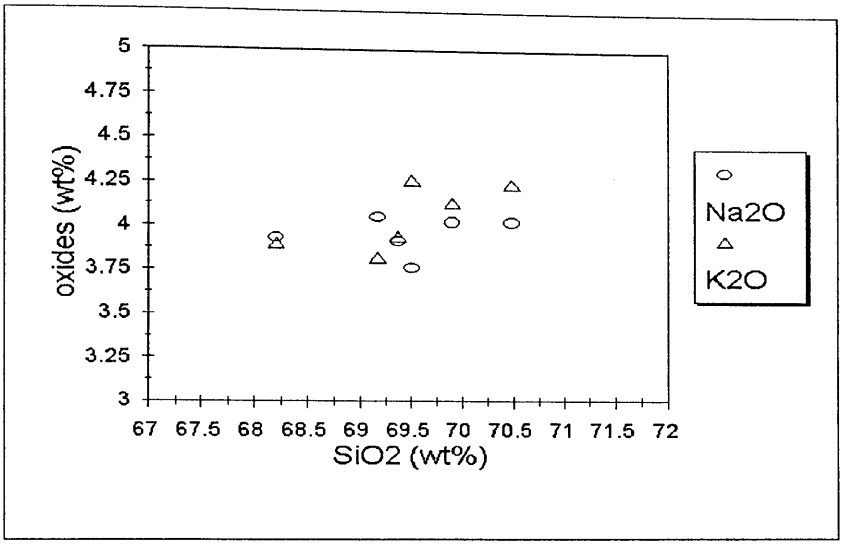

Figure 10.7: Na_2O and K_2O versus SiO_2 variation diagram of the Tchinhadzandze Granodiorite Gneiss.

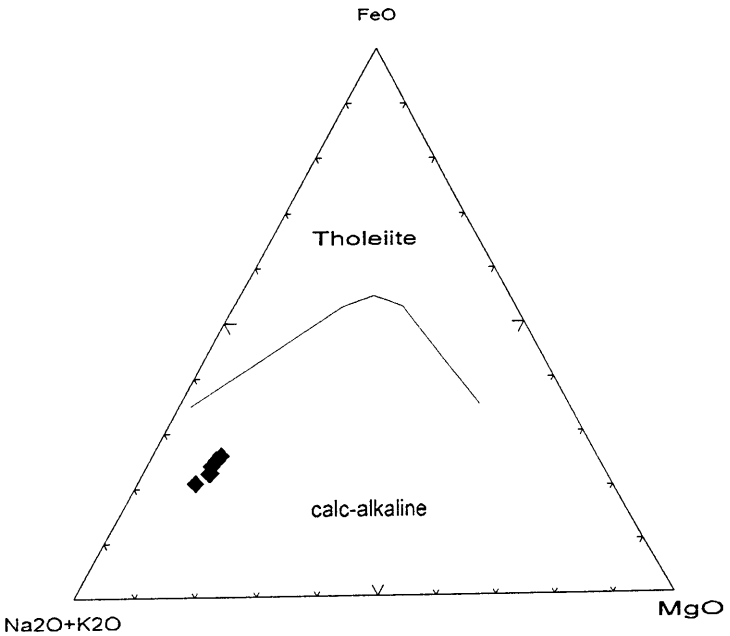

Figure 10.8: Irvine and Baragar (1971) discriminant diagram of the Tchinhadzandze Granodiorite Gneiss. Analyses plot in the field of calc-alkaline.

10.4.3 Trace Element Chemistry

In general the samples show little variation in their trace elements contents. Sr/Rb ratios are high resulting from the relatively low Rb contents and show a systematic variation between ~6:1 and ~7:1. Trace element spidergrams exhibit a pattern characterized by Rb, Ba, K and Sr enrichment relative to Nb, Zr, Ti and Y. This pattern is typical of volcanic-arc granitic magmas (Pearce *et al.*, 1984) (Fig. 10.9).

Two samples were analysed for their contents in rare earth elements (REE) (Table 10.3). The REE contents in this granite are characterized by a relatively high Ce, La and Nd values . The REE patterns for the two samples are shown in Fig. 10.10. The normalizing values are from Evenson *et al.* (1978).The REE patterns are characterized by enrichment of light rare earth elements relative to heavy ones with La_{cn}/Yb_{cn} of ~100, a weak positive Eu anomaly and a flat pattern of the heaviest elements Er, Yb and Lu. The positive Eu anomaly is possibly due to accumulation of Ca-feldspar. The flat HREE pattern may reflect hornblende accumulation in the source rock because the HREE are strongly partitioned into hornblende (Rollinson, 1993).

Table 10.3: Rare earth Element analyses of Tchinhadzandze Granodiorite Gneiss in ppm.

sample	La	Ce	Pr	Nd	Sm	Eu	Gd	Dy	Ho	Er	Yb	Lu
YGR1	38.01	76.27	7.8	25.93	3.48	1.25	2.23	1.24	0.19	0.41	0.39	0.06
YGR2	44.38	104.82	8.98	29.92	4.41	1.27	2.86	1.79	0.29	0.58	0.58	0.08

10.5 Discussion and Conclusion

The Ba-Rb-Sr contents of the Tchinhadzandze rocks are typical of granodiorites (El Bouseilly and El Sokkary, 1975) (Fig. 10.11) and the low Rb contents are typical of granitoids found in volcanic-arc settings (Pearce *et al.* 1984) (Fig. 10.12).

In conclusion, the Tchinhadzandze rocks have normative and chemical compositions of a granodiorite and the random orientation of of the planar fabric in this granite may indicate that the fabric is a flow fabric developed during emplacement.

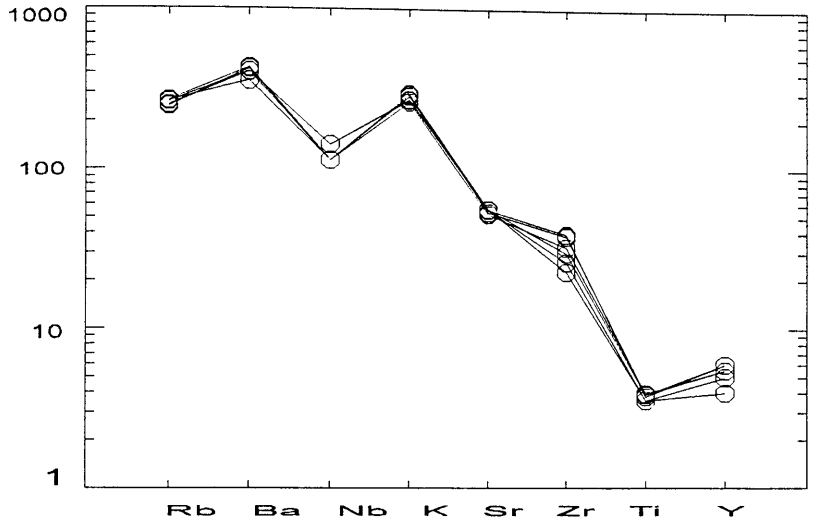

Figure 10.9: Chondrite normalized trace elements abundance variation diagram of Tchinhadzandze Granodiorite Gneiss (normalizing values after Sun, 1980).

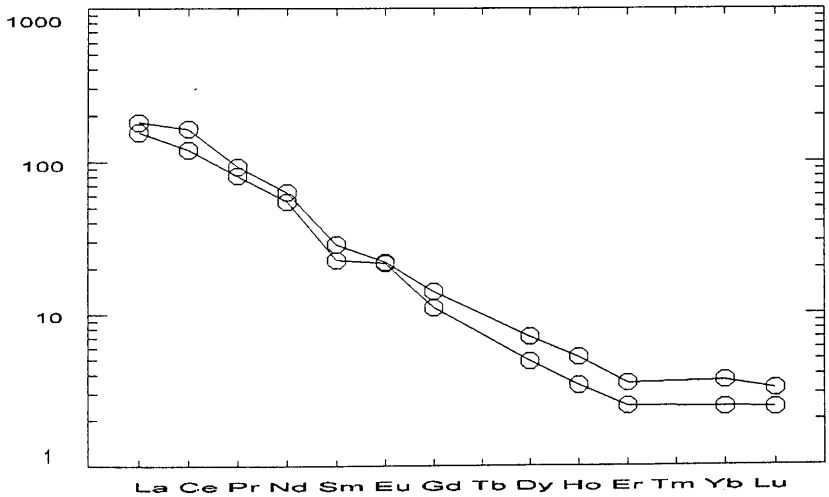

Figure 10.10: Chondrite normalized REE abundance variation diagram of Tchinhadzandze Granodiorite Gneiss (normalizing data after Evenson *et al*. 1978).

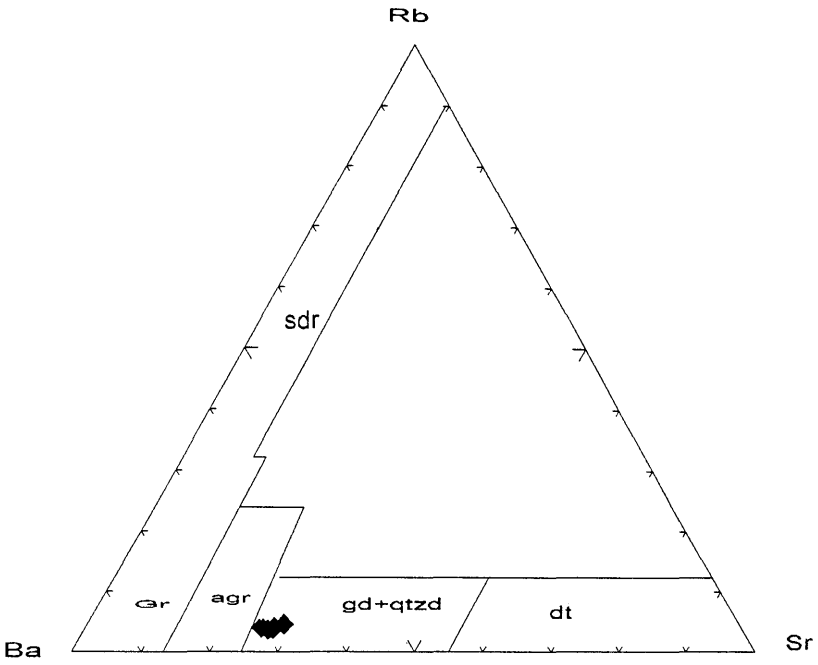

Figure 10.11: Diagram plotting samples in the field of granodiorites and quartz-diorites (after El Bouseily and El Sokkary, 1975). Sdr- strongly differentiated granites, Gr-normal granites, agr- anomalous granites and dt- diorites.

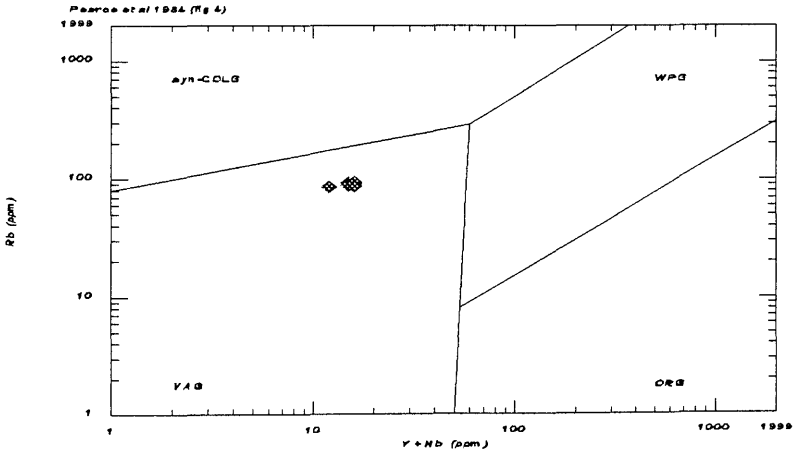

Figure 10.12: Pearce *et al.* (1984) tectonic discriminant diagram for granitoid rocks plotting the samples in the field of VAG (volcanic-arc granitoids). Syn-COLG- syn collisional, WPG- within plate, ORG- orogenic granites.

Chapter 11

STRUCTURAL GEOLOGY

11.1 Introduction

The study area can be subdivided into four structural domains labelled 1 to 4 and shown on the map (Fig. 11.1). The map displays rose diagrams of planar fabric strike directions. Figure 11.1 and the accompanying stereonets (Figs. 11.2, 11.3, 11.4, 11.5, 11.6, 11.7, 11.8, 11.9, 11.10, and 11.11) were prepared using the computer program Spheristat.

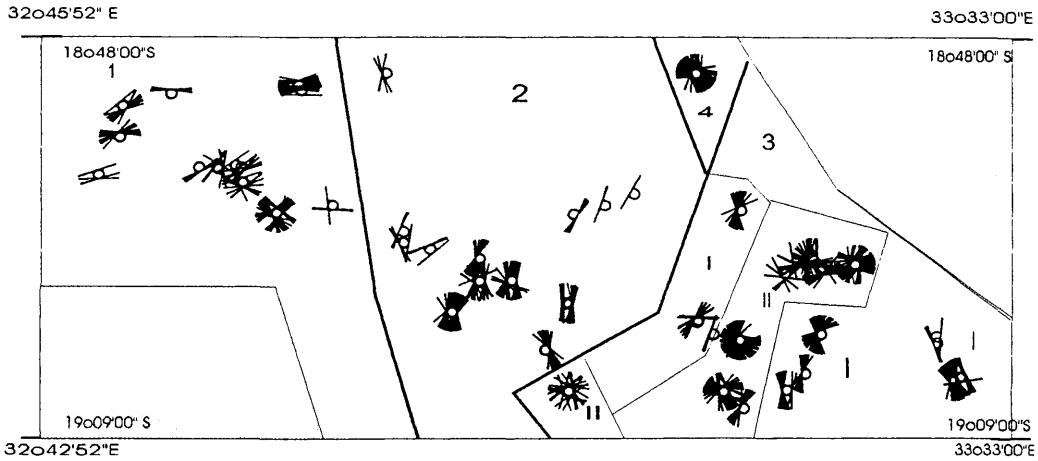

Figure 11.1: Map showing planar fabric strike directions and the subdivision of the study area in domains labelled 1 to 4. Within domain 3, sectors I and II are indicated. In grey are areas not covered by the study. The dimensions of the area are ~(37X88) km^2

11.2 Description of Structures

11.2.1 Domain 1

Comparison of Fig. 11.1 and 2.1 shows that this domain is underlain by the Manica Greenstone Belt and the Vumba Granite Gneiss. Stereonets 11.2, 11.3 and 11.4 represent the planar and linear fabrics measured in the Manica Greenstone Belt, the Vumba Granite Gneiss and the M'Beza/Vengo Formation respectively. The planar fabrics measured include the schistosity in the schists of the Manica Greenstone Belt, the foliations in the Vumba Granite Gneiss and the sedimentary layering in the M'Beza/Vengo Formation. Consequently they include S_o and S_1. The linear fabrics include mineral lineations (Fig. 11.2) and fold axes (Fig. 11.4). The axial plane foliations strike E-W to NE-SW with steep dips to the N and S and NW and SE (Figs. 11.2,11.3 and 11.4). The mineral lineations have a constant trend characterized by plunges of 60° towards 108° in average (Fig. 11.2) and the fold axes have plunges of ~30° towards E (Fig. 11.4). The schistosity has resulted from at least two kinds of movements, namely, a N-S compression and a dip/oblique-slip movement in a SE-NW direction and associated with the steeply dipping lineation (Fig. 11.2). The E-W oriented fold axes suggest that the

folds in the M'Beza/Vengo Formation (Fig. 11.4) were the result of N-S compressional movements.

Two stages of deformation took place, namely, D_1 which involved the development of planar fabrics parallel to primary layering resulting in S_o and S_1 having similar orientations. These fabrics were then folded by D_2 about axes which plunge shallowly to the east at ~30° suggesting N-S compression. Fig. 2.1 shows however that the strike of the foliation in the eastern sector of the Manica Greenstone Belt swings towards a NE-SW orientation.

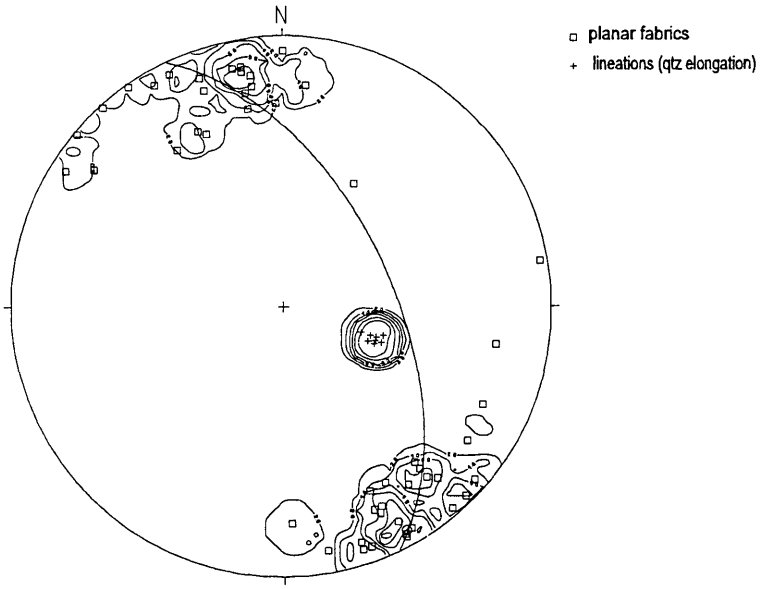

Figure 11.2: Poles to planar fabrics in the Manica Greenstone Belt and quartz elongation lineation in the quartz-sericite schist.

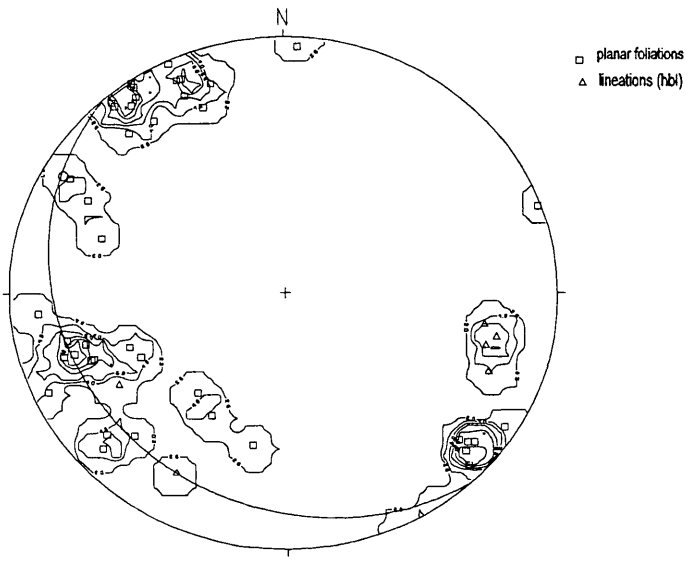

Figure 11.3: Poles to planar fabrics and mineral lineations in the Vumba Granite Gneiss.

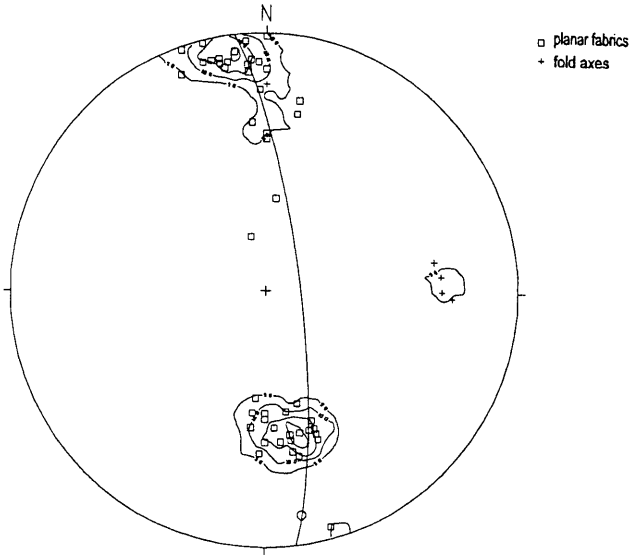

Figure 11.4: Poles to layering and schistosity and fold axes measured in the M'Beza/Vengo Formation.

11.2.2 Domain 2

Comparison of Figures 11.1 and 2.1 shows that this domain is underlain by the Messica Granite Gneiss and the Frontier Formation. Stereonets in Figures 11.5 and 11.6 represent the structural measurements from the Messica Granite Gneiss and the Frontier Formation respectively. In the gneiss, the measured structures are planar fabrics defined by the preferred orientation of biotite and hornblende, and linear elements defined by quartz grains elongation with sub-horizontal plunges towards the north (Fig. 11.5). In the metasediments of the Frontier Formation, the planar fabrics are primary layering (S_o) and foliation (S_1), defined by the development of metamorphic layering. The S_o and S_1 have similar to cross-cutting orientation at small angles. The foliation strikes are dominantly N-S with steep dips towards E and W (dominantly) (Figs. 11.5 and 11.6). The lineation has shallow plunges towards N. The steep planar fabric with associated near-horizontal mineral lineation suggests a N-S strike-slip environment (Hobbs *et al.* 1976, Passchier *et al.*, 1990).It is significant that the E-W planar fabrics in domain 1 are not seen in domain 2 which suggest that these fabrics possibly predate those in domain 2.

11.2.3 Domain 3

Comparison of Figures. 11.1 and 2.1 shows that this domain is underlain by the Vanduzi Migmatite Gneiss, the Nhansipfe Granite Orthogneiss and the Chimoio Granodioritic Gneiss. The stereonet in Figure 11.7 represenst the leucosomes, planar and linear fabrics measured in the Vanduzi Migmatite Gneiss. Stereonets in Figures 11.8 and 11.9 display the data for the planar and linear fabrics respectively, measured in the Nhansipfe Granitic Orthogneiss. The stereonet in Figure 11.10 shows the planar and linear fabrics measured in the Chimoio Granodioritic Gneiss.

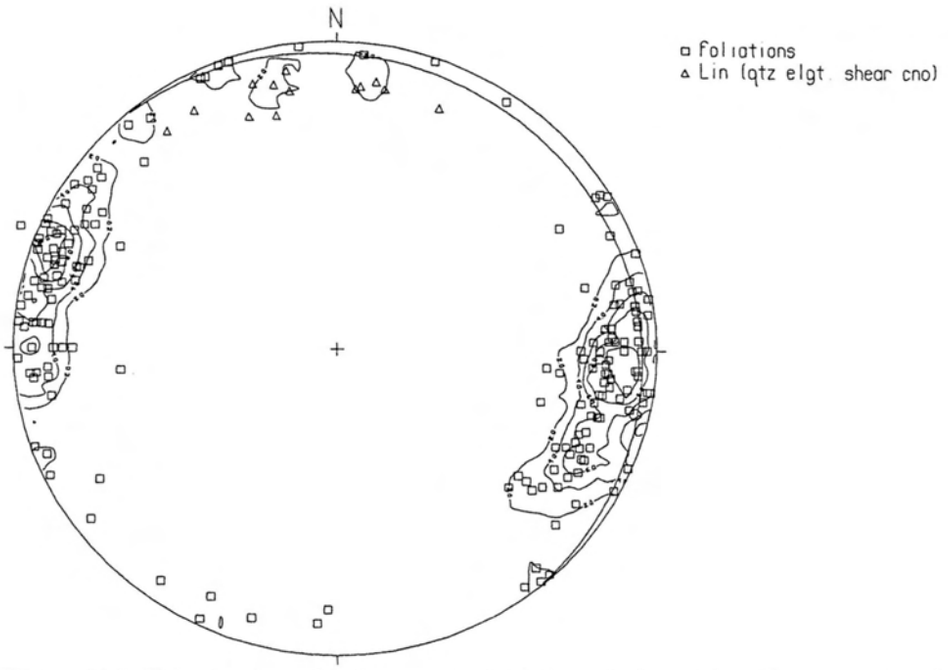

Figure 11.5: Poles to planar foliations and orientation of mineral lineations measured in the Messica Granite Gneiss.

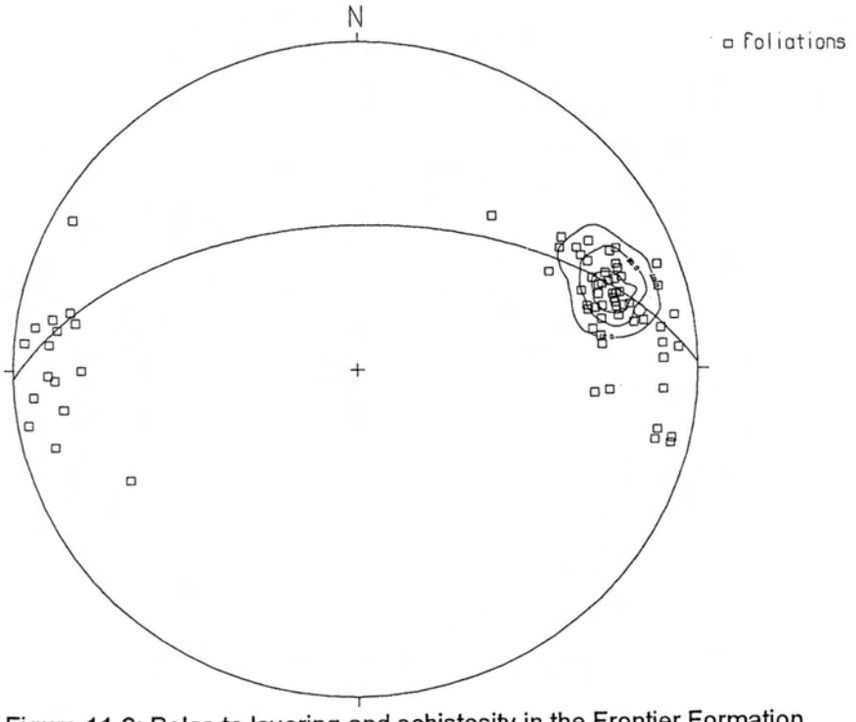

Figure 11.6: Poles to layering and schistosity in the Frontier Formation

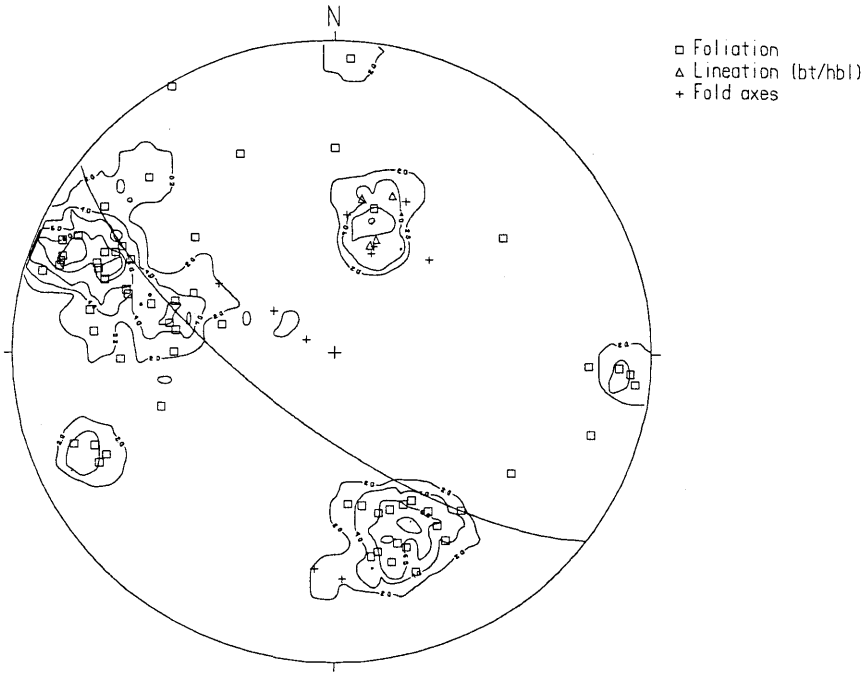

Figure 11. 7: Poles to planar fabrics and lenticular leucosomes and plunge directions of mineral lineations and fold axes in the Vanduzi Migmatite Gneiss.

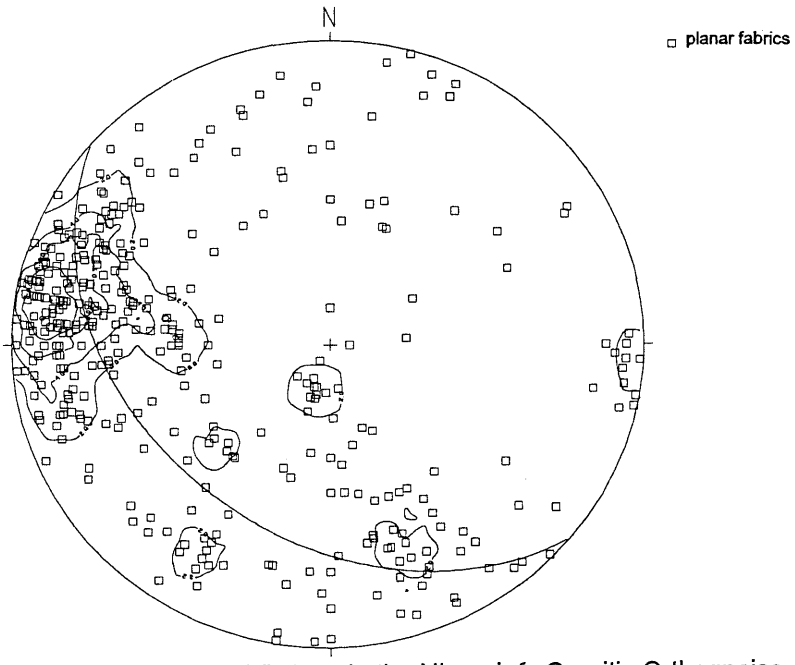

Figure 11.8: Poles to foliations in the Nhansipfe Granitic Orthogneiss.

In the Vanduzi Migmatite Gneiss planar fabrics comprise the primary layering S_0 and two foliations, namely, S_1 with E-W strike and moderate to steep dips towards N and S_2 with N-S strike and steep dips towards E and W. Two sets of leucosomes, correlated with S_1 and S_2 foliations are developed. The linear elements comprise mineral lineations and fold axes. These lineations and fold axes have essentially moderate plunges towards N. (Fig.11.7). The interpretation of this set of structural data suggests that D_1 involved the development of leucosome and planar fabrics parallel to primary layering to result in stage 1 leucosome, S_0 and S_1 having similar orientations. These planar fabrics as well as the leucosome were then folded by D_2 about axes which plunge ~45° towards N by a E-W compression. Apart from the S_2 foliation, the D_2 deformation is also associated with the development of strongly oriented N-S leucosomes. The moderately N plunging mineral lineation, suggests the occurrence of a N-S strike-slip movement.

In the Nhansipfe Granitic Orthogneiss planar fabrics (Fig.11.8) comprise mineral foliations defined by deformed feldspar megacrysts, biotite and hornblende whereas the linear fabrics are mineral lineations and fold axes (Fig. 11.9). The foliation is highly variable with a high concentration with N-S strikes and steep easterly dips. The lineations plunge shallowly to steeply to the NNE. The fold axes have variable orientations which lie crudely along a great circle which strikes NNE (~20°) and dips ~70° ESE.

The stereonet in Figure 11.10 represents planar and linear fabrics measured in the Chimoio Granodiorite Gneiss. The planar fabrics comprises mineral foliations defined by planar orientation of biotite and hornblende and essentially have N-S strikes and steep dips to E and W. Linear fabrics comprise mineral lineations defined by hornblende and biotite, and fold axes which plunge shallowly and moderately, respectively, to the N and S. These observations may suggest that the steep zones have originated from strike-slip deformation.

From Figure 11.1, Domain 3 can be subgrouped into subdomains I and II types. Type I subdomains are characterized by planar fabrics with dominantly N-S strikes. In subdomain type II, the planar fabrics have highly variable strikes. The wide range of foliations is also due to the recognition in the migmatite gneiss terrane of two generations of leucosome development, the first being oriented parallel to S_1 layering which is deformed and folded by S_2 which is oriented N-S. The second leucosome development is oriented N-S.

11.2.4 Domain 4

Comparison of Figure 11.1 and Figure 2.1 shows that this domain is underlain by the plutons of the Tchinhadzandze Granodiorite Gneiss.

Both planar and linear fabrics in these granites are weakly developed and variable. The poles to mineral foliations defined by biotite and hornblende show weak concentrations suggesting a NW-SE planar fabric (Fig. 11.11). The randomness of these foliations may also indicate that the fabric has resulted from primary magmatic flow. The lineations were measured in biotite and hornblende.

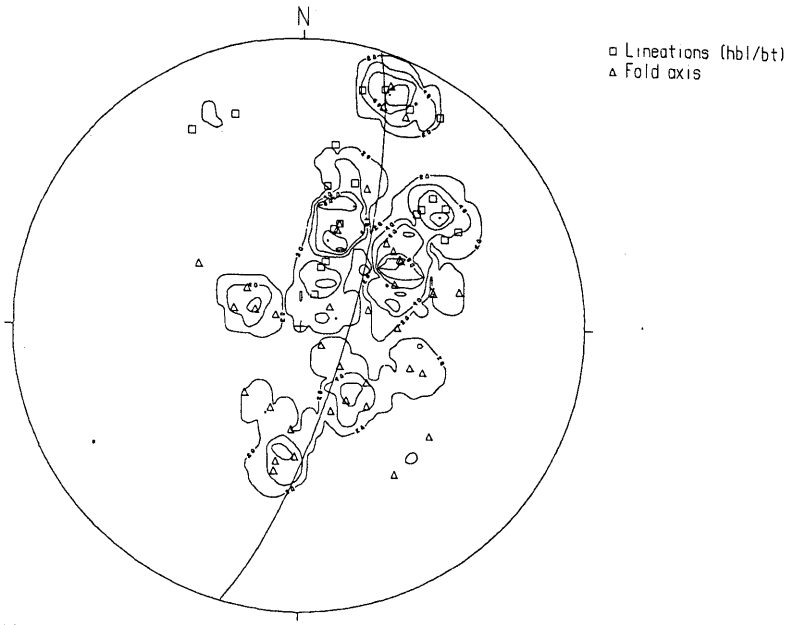

Figure 11.9: Mineral lineations and fold axes measured in the Nhansipfe Granitic Orthogneiss.

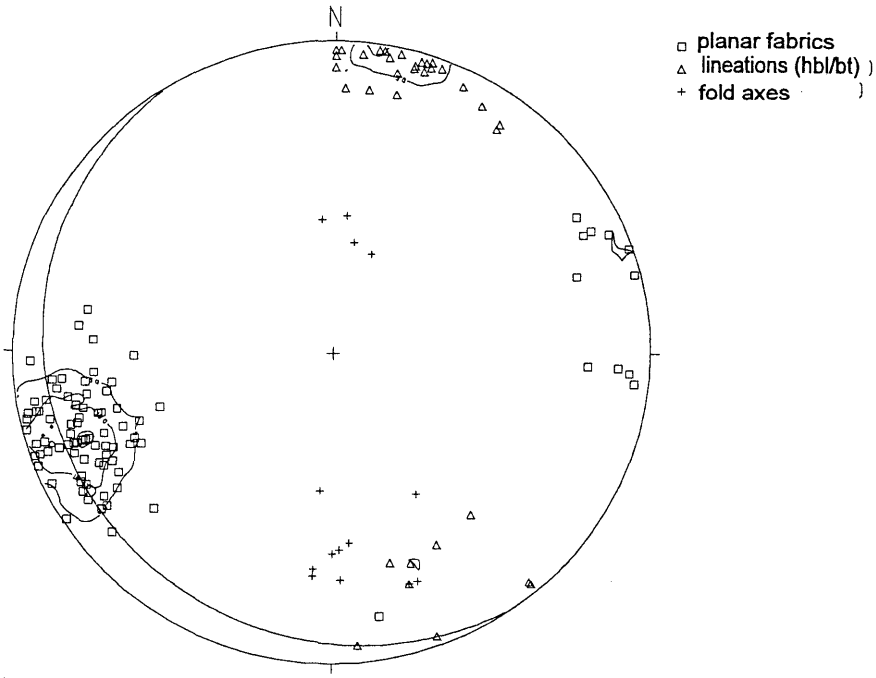

Figure 11.10: Poles to mineral foliations, mineral lineations and fold axes measured in the Chimoio Granodioritic Gneiss.

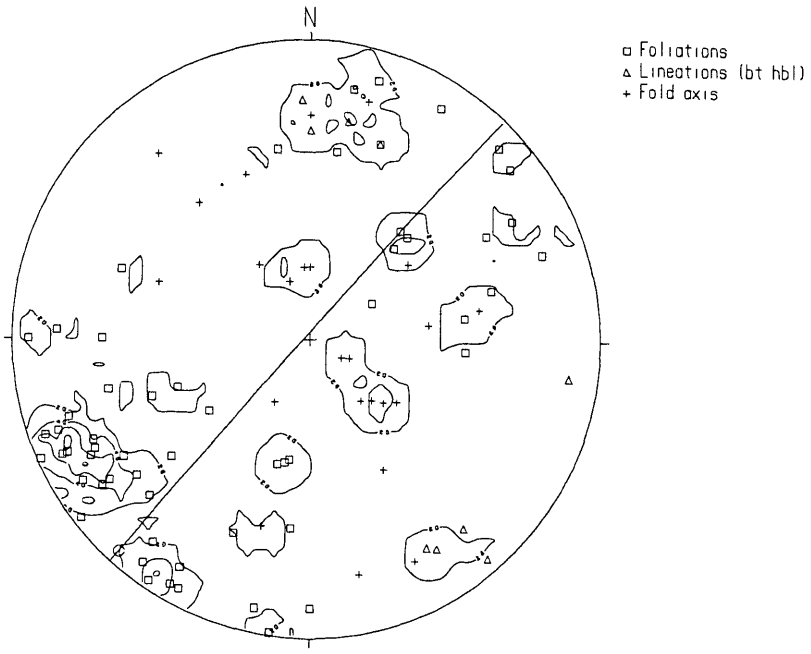

Figure 11.11: Poles to mineral foliations, mineral lineations and fold axes measured in the Tchinhadzandze Granodiorite Gneiss.

11.3 Conclusions

The study area is characterized by structures pertaining, on one hand, to the cratonic Granite-Greenstone Belt and structures pertaining to the Mozambique Metamorphic Province, on the other hand. Structures from the cratonic belt are not traceable into the Mozambique belt. This may suggest that the two belts may have been affected by different deformational episodes.

Within the greenstones, D_1 involved the development of planar fabrics parallel to primary layering which resulted in S_o and S_1 having similar orientation. A latter D_2 folded these planar fabrics about axes plunging shallowly (~30°) to the E suggesting a N-S compression and the steep mineral lineations with plunges towards ESE suggesting a dip-slip movement in an ESE-WNW direction.

Away from the craton, the structures become more complex as one progresses towards E. Thus, within the area underlain by the Messica Granite Gneiss and the Frontier Formation, planar fabrics have strikes essentially oriented N-S and steep dips to E and W. In the Frontier Formation the planar foliations are sub-parallel to primary layering.

Within the Mozambique Belt, two deformational episodes are recorded in the Vanduzi Migmatite Gneiss, east of Messica Granite Gneiss. D_1 is associated with development of planar fabrics parallel to primary layering and the development of planar leucosomes with strikes oriented E-W and steep to moderated dips towards N and S. D_2 folded these planar fabrics about axes that plunge ~45° towards N in a E-W compressional movement and is associated with the development of second stage planar

leucosomes. Towards the E, within the area underlain by the Nhansipfe Granitic Orthogneiss, the planar fabrics are highly variable but show a high concentration with N-S strikes. Present data suggest that the wide range of foliation may be associated with the existence of the two generations of leucosome development because away, in the Chimoio Granodioritic Gneiss the planar fabric have strikes with essentially NNW-SSE orientation. The steep planar fabrics associated with the shallowly to moderately plunging mineral lineations and fold axes in the Chimoio Granodiorite Gneiss, suggests the occurrence of strike-slip deformation.

Chapter 12

METAMORPHIC HISTORY

12.1 Introduction

Petrographic, geothermobarometric and thermochronologic data are used to constrain the metamorphic history of the study area. The area can be subdivided into a low grade metamorphic terrain and a medium- to high grade metamorphic terrain. The low grade terrain includes rocks belonging to the Archaean Greenstone Belt, the Vumba Granite Gneiss and the Early Proterozoic Messica Granite Gneiss. The medium- to high-grade terrain contains rocks of the Mid-to Late Proterozoic Frontier Formation, Vanduzi Migmatite Gneiss, Chimoio Granodioritic Gneiss and the Nhansipfe Granitic Orthogneiss and the Mafic Intrusions.

12.2 Metamorphism

12.2.1 Low Grade Terrain

The rocks in the Manica Greenstone Belt are characterized by a mafic to ultramafic suite containing chlorite+carbonate+serpentine+talc+tremolite+magnetite and a pelitic suite characterized by the quartz+sericite+chloritoid+chlorite+andalusite+fuchsite. Temperatures and pressures of metamorphism were constrained using Figures 3.10 and 3.11 which show that the mineral assemblage above are stable below 500 °C at 2 kbar. The coexistence of carbonate (dol) mostly+talc+serpentine in some samples (eg. mc, scg, 8) suggests that the fluid phase during metamorphism was a mixture of H_2O and CO_2 with $XCO_2 < 0.14$ which is characteristic of low grade or greenschist metamorphism. In the pelitic association, the occurrence of andalusite constrains the pressures of metamorphism below 3.8 kbar and temperatures above 400 °C below which pyrophyllite would be stable. The occurrence of chloritoid suggests temperatures below 525 °C above which it would be replaced by staurolite (Yardly, 1989, p. 86) (Figure 3.12).

Considering the intercalated nature of the pelitic and mafic to ultramafic schists, their combined mineral assemblages suggest P-T conditions of between 400-500 °C, 3.8 Kbar and mixed H_2O-CO_2 with $XCO_2<0.14$, typical of low grade or greenschist facies metamorphism. The occurrence of chloritization, saussuritization, as well as sericitization in the granitoids provides evidence of hydration reactions at low grade. The mineralogical assemblages dominated by Plg+Cpx+Act+Chl+Ep in the mafic intrusions within the Granite-Greenstone Belt are characteristic of basic rocks that have undergone low grade metamorphism of greenschist facies to greenschist-amphibolite transition facies (Bucher and Frey, 1994, p. 263, 273) (Fig. 9.7). The P-T diagram in this figure displays prograde metamorphic evolution of mafic rocks at various geotherms which is represented by chemographic ACF diagrams. The mineral assemblage of the mafic intrusions in Manica is compatible with chemographies 3 to 5.

12.2.2 Medium to High Grade Terrain

High grade rocks occur towards the E of the Granite-Greenstone Belt where the main outcrops are located in the Garuzo-Messica and Mombeza areas (Fig. 2.2). The mineral association include Plg+K-fld+Hbl+Bt, Plg+K-fld+Bt+Grt and Plg+K-fld+Hbl+Bt+Grt in the granitoids and migmatites and Plg+Hbl+Grt±Ilm, Plg+Hbl+Cpx and Plg+Hbl+Cpx±Opx+Grt in the mafic intrusions and enclaves. In the pelitic schist and quartzite of the Frontier Formation in Garuzo and Chimezi the assemblages are Qtz+Bt+Sil+Grt+Ms and Qtz+Sil+Ky+M respectively. In the pelitic schist the assemblage (Bt+Sil+Grt) in presence of quartz and muscovite (Fig.5.5) is typical of upper medium- to high-grade metamorphism (Winkler, 1974, p. 216) or upper amphibolite facies (T=~680 °C; P=~8 kbar) (Bucher and Frey, 1994, p. 273, 279). The application of computer program of Powell and Holland (1988) using present study data, gives a Ky-And-Sil triple point of P=~4.9 kbar and T=~582 °C. In the granitoids the mineral associations with garnet are typical of medium grade metamorphism and in the study area typically occur in the megacrystic granite. In the other granitoids the medium- to high grade metamorphism is supported by the occurrence of bands of partial melts associated with the gneisses. Their nature defines the migmatite gneiss as high grade terranes which in the present study is supported by the presence of garnet in the bands of leucosome supporting the occurrence of metamorphism at high grade. The associations Plg+Hbl+Grt±Ilm, Plg+Hbl+Cpx and Plg+Hbl+Cpx±Opx+Grt in the mafic intrusions and inclusions are characteristic of basic rocks that have been subjected to medium- to high-grade metamorphism (Bucher and Frey, 1994, p. 273, 279) (Fig. 9.7) and P-T conditions are constrained at ~5-8 kbar and ~750-800 °C.

12.3 Thermobarometry

12.3.1 Introduction

Sampling localities as well as sample coordinates are shown in Figure 2.2 and Appendix 1 respectively. Where applicable, the following activities and mineral formula recalculations models were used for the purpose of thermobarometry. Clinopyroxene and orthopyroxene activities were calculated after Wood and Banno (1973), garnet activities after Berman (1990), amphibole end-members activities after Kohn and Spear (1989, 1990) and plagioclase activities after Fuhrman and Lindsley (1988). The mineral formula and cation site allocations in amphibole and pyroxenes were determined using a MINPET 2.02 program. The analytical data used for the thermobarometry are summarized in Table 12.1 and complete microprobe data are shown in Appendix 2. The thermobarometric results are presented in Figures 12.1, for Garuzo-Chibata area (curves 1 to 5) and 12.2, for Mombeza area (curves 6-21). The data used for the construction of curves in this figure are given in Table 12.2 together with other thermobarometric data.

Table 12.1: Summary of analytical data used in thermobarometry.

Amphiboles

Sample	Maamp	Maamp	Maamp	Maamp	mxc	mxc	mbamp	mbamp	mbamp
Analysis	11	14	18	20	6	9	15	45	46
SiO_2	48.72	49.22	49.07	47.75	41.72	42.33	42.01	42.17	42.18
TiO_2	0.84	0.74	0.81	0.94	2.1	1.95	2.21	1.93	2.09
Al_2O_3	7.37	7.44	7.54	8.36	10.49	10.46	11.9	12.22	11.99
FeO	16.27	16.82	16.49	16.84	22.05	21.86	21.09	20.37	20.4
MnO	nd	nd	0.13	0.17	0.14	0.1	0.14	0.12	0.14
MgO	11.14	11.45	11.16	10.65	6.76	6.88	7.85	8.13	8.17
CaO	11.74	11.63	11.71	11.61	11.51	11.44	11.22	11.36	11.2
Na_2O	0.94	0.99	0.82	1.17	1.39	1.23	1.62	1.63	1.68
K_2O	0.59	0.53	0.56	0.64	1.39	1.5	ND	ND	ND
Si	7.192	7.183	7.192	7.05	6.468	6.529	6.38	6.387	6.395
[4]Al	0.808	0.817	0.808	0.95	1.532	1.471	1.62	1.613	1.605
[6]Al	0.473	0.462	0.493	0.503	0.383	0.429	0.509	0.566	0.536
Ti	0.093	0.081	0.089	0.104	0.245	0.226	0.252	0.22	0.238
Mg	2.451	2.491	2.438	2.344	1.562	1.582	1.777	1.836	1.847
Fe2+	2.009	2.053	2.021	2.079	2.859	2.82	2.461	2.378	2.379
Mn	0	0	0.016	0.021	0.018	0.013	0.018	0.015	0.018
sum oct	5.026	5.087	5.057	5.051	5.067	5.07	5	5	5
Ca	1.857	1.818	1.839	1.837	1.912	1.891	1.826	1.844	1.82
Na[M4]	0.117	0.095	0.103	0.111	0.02	0.04	0	0	0
Na[A]	0.152	0.185	0.13	0.224	0.398	0.328	0.477	0.479	0.494
K	0.111	0.099	0.105	0.121	0.275	0.295	0	0	0
Sum_A	0.263	0.284	0.235	0.344	0.673	0.623	0.477	0.479	0.494
Sum_cat	15.263	15.284	15.235	15.344	15.673	15.623	15.538	15.54	15.539

Garnets

Sample	Analysis	XGrs	XAlm	XPy	XSps
gcmx	5	0.039	0.872	0.059	0.03
gcmx	9	0.044	0.871	0.055	0.031
MaAmp	12	0.238	0.619	0.121	0.022
MaAmp	2	0.229	0.635	0.112	0.024
MaAmp	20	0.203	0.648	0.124	0.024
MaAmp	9	0.229	0.633	0.111	0.027
mxc	3	0.19	0.675	0.104	0.031
mxc	5	0.197	0.666	0.108	0.029
mxc	8	0.195	0.664	0.11	0.031
mbamp	21	0.197	0.646	0.122	0.034
mbamp	22	0.196	0.647	0.125	0.033
mbamp	33	0.206	0.641	0.123	0.03
mbamp	34	0.206	0.639	0.124	0.032
mbamp	15	0.202	0.66	0.107	0.031
mbamp	12	0.198	0.657	0.117	0.028
mbamp	11	0.204	0.653	0.114	0.03
mbamp	45	0.207	0.657	0.102	0.035
mbamp	46	0.196	0.642	0.127	0.035

Orthopyroxenes

sample	Analysis	XWo	XEn	XFs	XJd	XAe
mbamp	33	0.01	0.41	0.58	0	0

mbamp	34	0.01	0.4	0.58	0	0

Clinopyroxenes

sample	Analysis	XWo	XEn	XFs	XJd	XAe
mbamp	21	0.45	0.3	0.25	0.04	0
mbamp	22	0.45	0.3	0.24	0.04	0
mbamp	11	0.44	0.3	0.26	0.04	0
mbamp	12	0.44	0.3	0.26	0.04	0

Ilmenites

Sample	Analysis	Mineral	Ti	Fe2	Mn	Mg
mxc	7	ilm	4.037	4.332	0.03	0.06
mxc	8	ilm	4.013	4.325	0.04	0.07

Plagioclases

Sample	Analysis	XAb	XAn	XOr
MaAmp	12	0.46	0.53	0.01
MaAmp	5	0.47	0.52	0.01
mbamp	13	0.6	0.38	0.02
mbamp	41	0.61	0.37	0.02
mbamp	43	0.59	0.4	0.02

ND- not determined and nd- not detected.

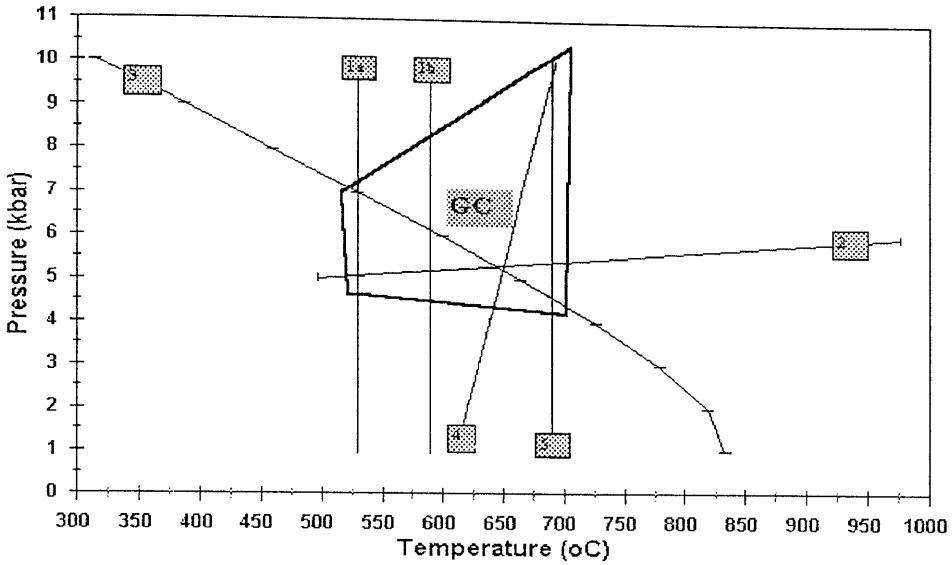

Figure 12.1: Thermobarometric results of mafic dykes and inclusions from the Garuzo-Chibata area, within the Mozambique Metamorphic Province. The prevalent P-T conditions are indicated by the polygon GC.

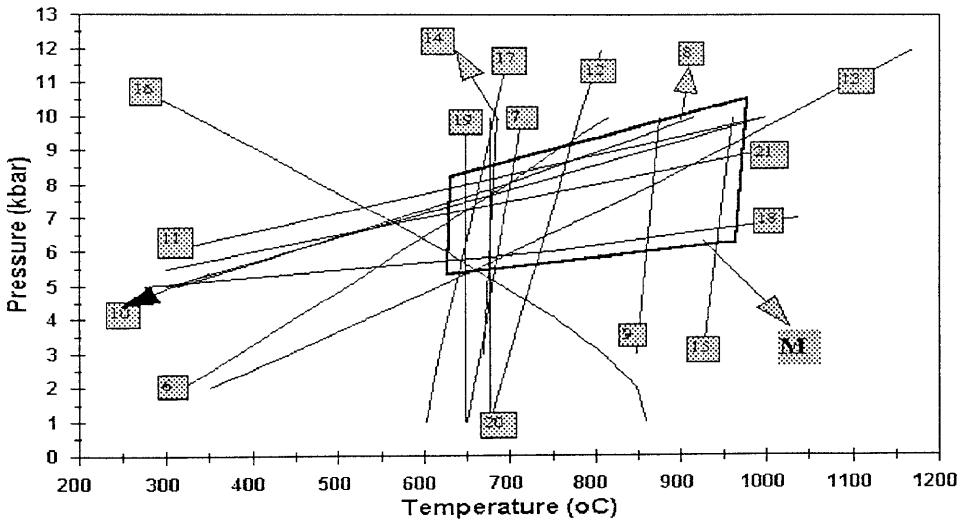

Figure 12.2: Thermobarometric results of mafic dykes from the Mombeza area, east of Chibata, within the Mozambique Metamorphic Province. The prevalent P-T conditions are indicated by the polygon M.

Table 12.2: Results of thermobarometric calculations.

Curve	Sample	Assemblage	T(°C)	P(kbar)
1a	maamp	Grt-Hbl*	529.09	5.1-8.08
1b	"	Grt-Hbl**	589.34	5.52-8.32
2	"	Hbl-Plg-Grt-Qtz	497-976	5-6
3	"	Hbl-Plg-Grt-Qtz	314-833	1-10
4	"	Hbl-Plg-Grt-Qtz	612-692	1-10
5	mxc	Grt-Hbl	690	1-11
6	Mbamp	Alm-Gr-Qtz-An-Hed	319-816	2-10
7	"	Di-Alm-Hed--Py	651-714	1-10
8	"	Py-Gr-Qtz-An-Di	314-917	5-10
9	"	Grt-Cpx	848-876	3-10
10	"	Grt-Cpx-Plg	300-1000	5-10
11	"	Grt-Cpx-Plg	300-1000	6-10
12	"	Hed-En-Alm-Di-Fs-Py	677-806	2-12
13	"	Hed-Alm-Qtz-An-Fs	352-1170	2-12
14	"	Cpx-Opx	670-685	3-10
15	"	Opx	927-961	3-10
16	"	An-Hbl-Py-Gr-Qtz-	256-859	1-11
17	"	Hbl-Alm-Py	602-699	1-12
18	"	Alm-Gr-Qtz-An-Hbl	275-1038	5-7
19	"	Grt-Hbl	648*	1-10
20	"	Grt-Hbl	676**	1-10
21	"	Grt-Hbl-Plg-Qtz	300-1000	5.5-9
	"	Grt-Hbl-Plg-Qtz	300-1000	5.27-10.58
	"	Grt-Cpx-Plg	300-1000	6.02-11.41
	"	Opx	906.23-977.72	
	"	CpX-Opx	635.91-684.69	8.10-12.36
	"	Grt-Cpx	833.13-852.74	3.97-9.37
	"	Grt-Hbl	676.79	5.53-9.13
	"	Grt-Hbl	648.05	5.68-9.00
	mxc	Grt-Hbl	620.34-688.84	5.5-9.22
	mxc	Grt-Ilm	610-645.6	5.41-8.64
	mbamp	Cpx-Plg-Qtz	300-1000	12.2-9

Curves 1-21 were used in the in the construction of the diagram of Figure 12.1. Shown also are other calculated thermobarometric data which were not used in the construction of the curves. *- determination after Perchuck *et al.* (1985); **- calculation after Graham and Powell (1984).

12.3.2 Thermometry

The mineral assemblages used for thermometry in present study include garnet-amphibole, garnet-ilmenite, garnet-clinopyroxene and clinopyroxene-orthopyroxene. Samples maamp, mxc and mbamp contain garnet and hornblende in apparent textural equilibrium and are, therefore, suitable for garnet-hornblende thermometry. The compositions of these minerals were used to estimate the temperatures applying the Graham and Powell (1984) and Perchuck *et al.* (1985) geothermometer calibrations.

In general the Perchuck *et al.* (1985) geothermometer gave relatively lower temperatures in comparison with the Graham and Powell (1984) geothermometer and were, therefore, used for the estimations of minimum temperatures. The thermometry results suggest that a temperature of between ~530 °C and ~570 °C (obtained from assemblages in sample maamp) and between ~620 °C and ~690 °C (estimated from sample mxc) prevailed during the metamorphism in areas around Garuzo-Messica

and Chibata (Fig. 2.1). In Figure 12.1 curves 1a and 1b are plotted using the lower and the higher temperatures obtained using both geothermometers for sample maamp, and curve 5 is plotted using the value from Graham and Powell (1984) for the sample mxc. Thermometry using compositions from sample mbamp from Mombeza area, in the east (Fig.12.2) yield temperature estimates between ~650 °C (curve 19) (Perchuck *et al.* 1985) and ~680 °C (curve 20) (Graham and Powell, 1984) which are higher than those from sample maamp but lower than those from sample mxc.

The sample mxc contains garnet and ilmenite and, therefore, is suitable for Grt-Ilm thermometry. Grt-Ilm geothermometers calibrated by Pownceby *et al.* (1987) and Pownceby *et al.* (1991) yield temperature estimates of ~640 °C and ~615 °C respectively which are slightly lower than those obtained using the Grt-Hbl geothermometer.

The sample mbamp contains the additional suitable assemblages Grt-Cpx, Grt-Opx, Cpx-Opx which were used to estimate the metamorphic temperatures. For the assemblage garnet+clinopyroxene, the Grt-Cpx geothermometer of Sengupta (1989) was used for temperature estimates and gave values between ~830 and ~880 °C whereas for clinopyroxene+orthopyroxene assemblage, the Cpx-Opx and Opx geothermometers of Brey and Kohler (1990) were applied and yielded values of ~670 °C to ~685 °C and ~910 °C to ~980 °C (Table 12.2) respectively. The Cpx-Opx estimates are only slightly higher than those obtained using Grt-Cpx geothermometers whereas the Opx estimates are the highest temperature estimates within the study area. In Figure 12.2, the Grt-Cpx geotherm of 848 °C-876 °C is plotted as curve 9 whereas that of Opx is plotted as curve 15. It is worth mentioning that the curves of these two geothermometers are concordant with the reaction geothermometers (curve 7) containing the assemblages, suggesting that these geothermometers are built up on the same equilibria and are, therefore, reliable temperature estimators.

12.3.3 Barometry

The assemblages used for barometry include garnet-amphibole-plagioclase-quartz, garnet-clinopyroxene-plagioclase and clinopyroxene-plagioclase-quartz. The equilibrium reactions comprising these assemblages were calculated using the computer program THERMOCALC (Powell and Holland, 1988). This program requires the knowledge of minerals end-members activities, which were computed as specified earlier.

For the garnet-amphibole-plagioclase-quartz assemblage, three intersecting reactions were calculated, namely, 9An+6Hbl->8Py+7Gr+15Qtz+H_2O (curves 3, 16), 3Hbl+4Alm->FHbl+4Py (curves 4,17) and 8Alm+7Gr+15Qtz+6 H_2O->An+6Fhbl (curves 2, 18). P-T conditions for the intersecting points are similar, being P=5.2 kbar and T=649 °C and P=5.7 kbar and T=643 °C in samples maamp (Fig. 12.1) and mbamp (Fig. 12.2) respectively. Pressure estimations for the assemblage garnet-amphibole-plagioclase-quartz were done according to Kohn and Spear (1989,1990). Although all samples (mxc, maamp and mbamp) contain the appropriate mineral assemblages, only the compositions of minerals from sample mbamp satisfied the compositional parameters set out in Kohn and Spear(1989,1990). The pressure estimates are ~6.0 kbar for T=300 °C and ~9 kbar for T=1000 °C. These data are plotted in Figure 12.2 as curve 21. The sample mbamp

also contains the assemblages garnet-clinopyroxene-plagioclase and clinopyroxene-plagioclase-quartz, and is, therefore, adequate for Grt-Cpx-Plg and Cpx-Plg-Qtz barometry. Using the computer program THERMOCALC (Powell and Holland, 1988), three intersecting reactions (at P=8 kbar and T=700 °C), two of which containing this assemblage, were determined, namely, Alm+2Gr+3Qtz->An+3Hed (curve 6), Py+2Gr+3Qtz->3An+3Di (curve 8) and 3Di+Alm->3Hed+Py (curve 7) (Fig.12.2).The Grt-Cpx-Plg geobarometer after Eckert *et al.* (1991) (curve 10) suggests pressures of ~5 and ~10 kbar for 300 and 1000 °C respectively, and that of Powell and Holland (1988) (curve 11) suggests similar pressures of ~6 and 10 kbar for the same temperatures. Estimations from Cpx-Plg-Qtz after Ellis (1980), however, provide values of ~12 kbar for T=300 °C and ~9 kbar for T=1000 °C (Table 12.2). From the Figure 12.2 it can be seen that curves 11 and 10 are convergent at high temperatures. The geobarometer almost cut through the intersection point suggesting, consequently, that it may be a good pressure estimator.

In conclusion, the thermobarometric study suggests an increase in P-T conditions during metamorphism within the Mozambique Metamorphic Province, from Garuzo-Chibata to Mombeza of ~5 to ~10 kbar and ~530 to ~980 °C.

12.3.4 Discussion of Petrographic and Thermobarometric Results

Estimations of P-T conditions in the low grade terrain are entirely constrained, using petrographical data, at between 400 and 525 °C and ~4 kbar. Petrographical data within the medium- to high-grade terrain constrain P-T conditions at P=~5 -~8 kbar and T= ~580 -~800 °C. Thermobarometry suggests P-T conditions of ~5 -~10 kbar and ~530 -~980 °C, a bracket which contains the estimations from petrography.

It can be concluded that the study area records a metamorphic history characterized by an increase in P-T conditions from the low-grade greenschist facies metamorphism in the W to the high-grade amphibolitic-granulite facies metamorphism in the E.

12.4 Thermochronology

12.4.1 Introduction

Thermochronological investigations were undertaken using the $^{40}Ar/^{39}Ar$ step heating method in 6 samples from the Vumba Granitoid Gneiss (V Gr2/P and Vgr-3b), the Messica Granite Gneiss (Pd Gr/P), the Chimoio Granodioritic Gneiss (Cv1 Gr/P), the Nhansipfe Granitic Orthogneiss (Nfg/P) and in quartzite from the Frontier Formation (Ch Qtz). Sample locations are shown in Fig. 2.2 and the co-ordinates in Appendix 1.

The step heating method is based on the formation of ^{39}Ar from neutron irradiated ^{39}K-bearing samples and give dates that are calculated from measured $^{40}Ar/^{39}Ar$ ratios. By using the incremental heating technique several dates can be obtained from a single sample by counting the released argon from it in steps of increasing temperature (Berger and York, 1981; Faure, 1986). Like any other radiogenic method, this one is also sensitive to any loss or gain of radiogenic argon because excess argon may give rise to older dates whereas the loss of argon will yield younger ages. In a closed

system, step heating should give rise to plateaus of identical dates and at least 50% of these plateaus should be present for the dates to be considered reliable ages. The ages thus obtainable are mineral closure ages and the method is applicable to dating K-bearing minerals such as biotite, muscovite, hornblende, K-feldspar and plagioclase. Because closure temperatures of these minerals are known, or can be obtained, ultimately the method gives data that can be used for the construction of temperature-time loops. Closure temperatures of the argon system in biotites are estimated at ~350 - ~400 °C (Berger and York, 1981) and in muscovites at ~350-~400 °C (Mezger, 1991).

For the purpose of present study, muscovite separates were extracted from the quartzite (ChQtz) whereas biotite separates were extracted from the granitoids. Samples Vgr2/P and Vgr-3b from the Archaean Vumba Granite Gneiss were selected with the aim of obtaining information on possible mineral resetting due to the Mozambique and Pan-African orogenies. For the younger Mozambique Belt granite gneisses and metasediments of the Frontier Formation, we seek information on possible later orogenies including the Pan-African. The laboratory investigations were conducted by Dr. P. Guise at the Department of Earth sciences, University of Leeds, Leeds, U. K. and the results are presented in Table 12.3 and the diagrams are shown in Figures 12.(A-F).

12.4.2 Discussion of Results

Diagrams in Figs 12.A and 12B show that the plateaus are characterized by weak fluctuations at just above 1000 Ma but no consistent plateaux were obtained. The total gas ages are 1084±4 Ma and 1067±4 Ma respectively and their similarity suggest that they are due to the same geological process. Argon data yield similar mineral resetting ages of 535±2.5 Ma and 558±2.5 Ma respectively in the Early Proterozoic Messica Granite Gneiss and in the Middle Proterozoic Chimoio Granodiorite Gneiss (Figs. 12.C and 12.D) and suggests that this mineral resetting was caused by the same geological event. Argon counts in the diagrams of Figures. 12.E and 12.F yield similar mineral resetting ages of 467±2 Ma and 468±2.7 Ma respectively in the Late Proterozoic Nhansipfe Granitic Orthogneiss and in the possible allochthonous Frontier Formation suggesting that the two units were affected by the same thermal process. It is significant that these younger ages are coincident with areas which have strong planar N-S fabrics. This suggests a degree of young re-activation along these zones.

Similarities between the mineral resetting ages in the Archaean granitoids and age of emplacement of the Nhansipfe gneisses of ~980±83 Ma suggest that the heat that caused the mineral resetting in the Archaean granitoids was possibly derived from the intrusion of Nhansipfe Granitic Orthogneiss. The ages in the metasediments and younger granitoids are consistent with the Pan-African orogeny time span of about ~550 Ma -~450 Ma. The age difference of about ~100 Ma observed in these units is geologically significant and suggests the occurrence of a localized thermal process at about ~460 Ma. This event is supported by the occurrence of a zone of extensive migmatites in the area (Fig. 2.1) and the intrusion of the syn-to post-tectonic Tchinhadzandze Granodiorite Gneiss.

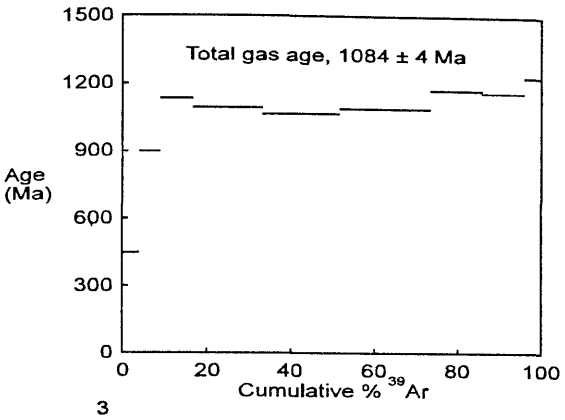

3

Figure 12.A: Cumulative Ar versus age diagram of Vumba granitoids.

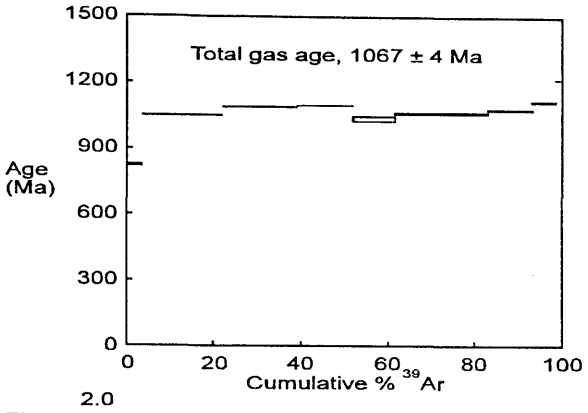

2.0

Figure 12.B: Cumulative Ar versus age diagram of Vumba granitoids.

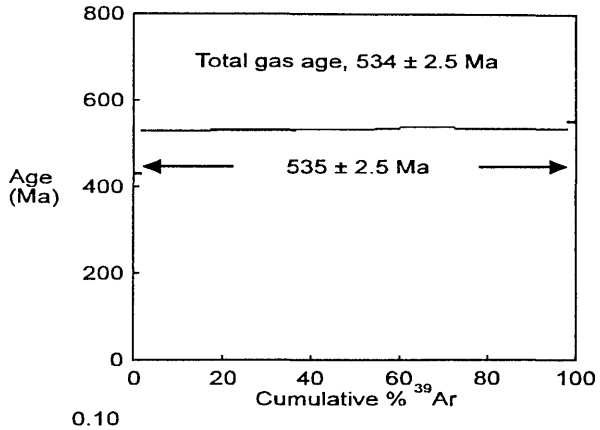

0.10

Figure 12.C: Cumulative Ar versus age diagram of Messica granitoids.

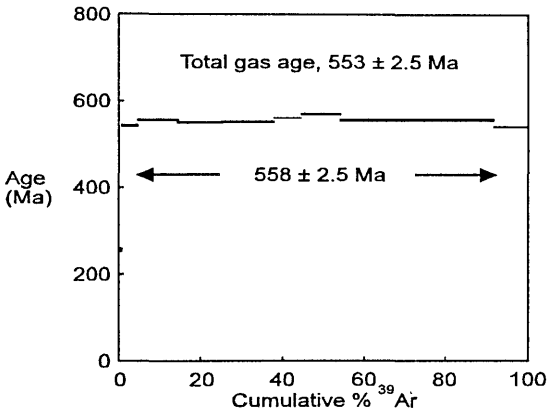

Figure 12.D: Cumulative Ar versus age diagram of Chimoio granitoids.

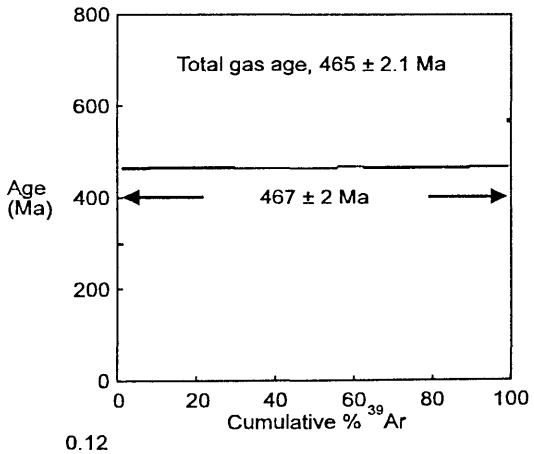

0.12

Figure 12.E: Cumulative Ar versus age diagram of Nhansipfe granitoids.

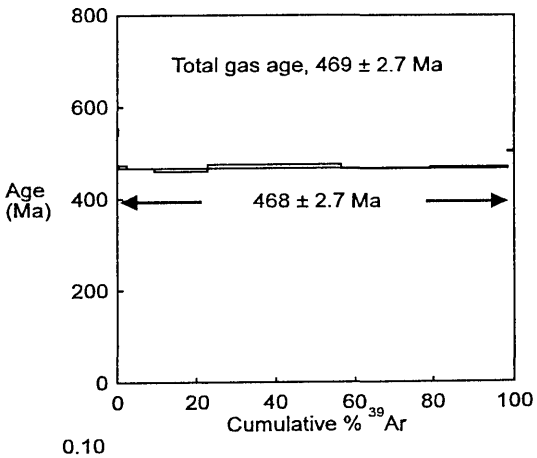

0.10

Figure 12.F: Cumulative Ar versus age diagram of the Frontier Formation quartzite.

Table 12.3: Thermochronological data of various lithological units.

Lithological unit	Mineral	Age (Ma)	Closure temperature (°C)
Barue Group	biotite	425±20[a]	350-400
Frontier Formation	muscovite	465±20[a]	"
Nhansipfe Granitic Orthogneiss	biotite	467±2	"
Frontier Formation	muscovite	468±2.7	"
Gairezi Group	biotite	526±30[a]	"
Messica Granite Gneiss	biotite	535±2.5	"
Chimoio Granodioritic Gneiss	biotite	558±2.5	"
Vumba Granite Gneiss	biotite	1067±4[b]	"
Vumba Granite Gneiss	biotite	1084±4[b]	"

([a]) after Vail(1965), ([b]) total gas age. Biotite and muscovite closure temperatures after Berger and York (1981) and Mezger (1991) respectively.

In conclusion, mineral resetting investigations by the $^{40}Ar/^{39}Ar$ method suggest that the Archaean Vumba Granite Gneiss was affected by a thermal event at about the same time the Nhansipfe Granitic Orthogneiss was intruded. Younger thermal events did take place between ~460 Ma and ~550 Ma in the Mozambique Belt, with the youngest thermal events only affecting a very localized zone, possibly in response to a later Pan-African related heating event. Closure temperatures of the systems are estimated at ~350-400 °C. The calculated mineral resetting ages are similar to those determined by K/Ar method in muscovite from quartzite of Frontier Formation in Chicamba (465 ± 20 Ma) within the study area, in biotite from gneiss (425 ± 20 Ma) and schist (526 ± 30 Ma) within the Barue and Gairezi Groups in Macossa and Gairezi respectively (Vail, 1965), localities which are located reasonably close and are geologically similar to the study area. They are equally correlatable to those determined in Antarctica (Grantham *et al.*, 1988; Grantham *et al.*, 1991 and Grantham *et al.*, 1995). These similarities suggest that the areas were affected by the same thermotectonic events.

12.5 Metamorphic History

The low grade greenschist metamorphism is the oldest metamorphism episode (M_1) overprinted in the study area and is mostly recorded in the Archaean greenstone rocks in the west (Fig. 2.1). The maximum P-T conditions were ~4 kbar and ~525 °C and as a result, low grade mineral paragenesis were formed. As a result of the Kibaran tectonothermal Mozambique Orogenesis during 950 - 1100 Ma (Petters, 1991, p. 15) areas towards the E (Fig. 2.1) were affected by the orogeny which along with deformation, submitted the rocks to medium-high-grade metamorphism (M_2) at P-T conditions of ~5-~10 kbar and ~530 -~980 °C). These P-T conditions did not affect the rocks in the low grade terrane where only mineral resetting is registered at about ~1100 Ma. The third (M_3) metamorphic episode is associated with the Pan-African orogeny which ended at ~450 Ma (Petters, 1991, p. 15: Pinna *et al.* 1993) and resulted in mineral resetting and, possibly, in granitoid emplacement such as the Tchinhadzandze Granodiorite Gneiss.

Chapter 13

SUMMARY OF CONCLUSIONS

13.1 Lithologies

The geology of the study area is essentially the geology of cratons and mobile belts. The cratonic areas are the Archaean Zimbabwe Province dominated by granite-gneisses and greenstone rocks, whereas the Proterozoic Mozambique Metamorphic Province is dominated by granitoids. This structural framework is consistent with the Precambrian geology of Southern Africa (Petters, 1991, p. 5).

The greenstone belt comprises the Macequece and the M'Beza/Vengo Formations. Rock types in the Macequece Formation include talc-chlorite schists, carbonate antigorite fels, quartz-sericite and chloritoid-andalusite schists, gabbroic rocks and felsic to mafic tuffs. The M'Beza/Vengo Formation comprises metaconglomerate, metagreywackes, pelitic schists, locally interlayered with conglomerates, greywackes, shales, mudstones and carbonate lenses. Chemically the mafic to ultramafic schists are peridotitic komatiites. Similar rock types are described in the greenstone belts of South Africa (Viljoen and Viljoen, 1969; Viljoen *et al.*, 1982) and in the greenstone belts of Zimbabwe (Wilson *et al.*, 1978).

The Archaean Vumba Granite Gneiss vary from metaluminous to peraluminous whereas the Early Proterozoic Messica Granite Gneiss is metaluminous. They vary from tonalites throughout the granodiorites to monzogranites and constitute the typical tonalite-trondjhemite-granodiorite (TTG) association common in the Archaean granitoids (Martin, 1987; Clarke, 1992, p. 198). The chemistry of Vumba Granite Gneiss is typical of mantle fractionates whereas that of the Messica Granite Gneiss is typical of a crustal melt. These characteristics are similar to those described in the Barbarton granite suite in South Africa and Swaziland by Viljoen and Viljoen (1969) and Hunter (1973) and in Zimbabwe by Wilson *et al.* (1978).

The Frontier Formation is, possibly, an allochthonous metasedimentary sequence comprising quartzite and pelitic schist units which were metamorphosed to medium grade amphibolite facies. Towards the northwest, the Frontier Formation is thrust over the greenstones. In this area the occurrence of kyanite in the schist suggests higher pressures than those in the underlying andalusite bearing greenschist. Although allochthonous, the Frontier Formation does not overlie the rocks of the Mozambique Metamorphic Province and, consequently could predate the Mozambique Orogeny.

The high grade Vanduzi Migmatite Gneiss is characterized by the development of two stages of leucosomes associated with respective gneissose planar fabrics. Petrographically, the leucosome are a Qtz±Fld±Bt±Hbl variety and a Grt+Qtz+Fld variety.

The Middle Proterozoic Chimoio Granodioritic Gneiss is banded and interlayered with amphibolitic and migmatite gneisses. The mineralogy of the gneiss is characterized by low proportions of quartz and structurally by the combination of zones of steep and shallow fabrics and is metamorphosed to medium grade amphibolite facies. It is metaluminous and has a chemical signature typical of

volcanic-arc granitoids and, consequently, this formation may be compared to the Jutulrora Formation in western H. U. Sverdrupfjella in Antarctica described by Grantham *et. al.* (1995) and Grantham *et al.* (1997).

The megacrystic A-type and Late Proterozoic Nhansipfe Granitic Orthogneiss has undergone metamorphism to medium grade amphibolite facies and local tectonic grain size reduction. The fact that partial melting is seen in these gneisses shows that they have been metamorphosed to high-grade but now have medium-grade assemblages. Mafic boudins included in this gneiss, preserve high grade granulite assemblages. The gneisses vary chemically from metaluminous to peraluminous and have had some trace elements redistributed by metasomatism which result in its plotting as anomalous granite in the classification diagram of El Bouseilly and El Sokkary (1975). These megacrystic gneisses may be similar to the Kirwanveggen Megacrystic Orthogneiss in the Dronning Maud Land , Antarctica (Grantham *et al.*, 1995).

The mafic rocks intruding rocks of the granite-greenstone belt are metamorphosed to greenschist facies and preserve an igneous texture whereas the mafic dykes intruding rocks of the Mozambique Metamorphic Province are metamorphosed to medium to high grade amphibolite up to granulite facies, and record granoblastic metamorphic textures and planar fabrics oriented N-S. Despite their differences in terms of petrography and the crust they intrude, the mafic rocks are chemically similar, being subalkaline and tholeiitic and have chemical signatures typical of ocean floor basalts. The mafic intrusions in Jutulrora, mainly, and Brekkerista and Roerkulten in Antarctica comprise N-S deformed and undeformed dykes (Grantham *et al.* 1988), with the metamorphosed ones having a Plg+Hbl+Grt amphibolite facies paragenesis and a planar foliation defined by oriented hornblende and biotite, resulting in these dykes being similar to the dykes within the Mozambique belt.

The Tchinhadzandze Granodiorite Gneiss comprises syn-to post-tectonic plutons that have undergone retrogressive hydration reactions. It is metaluminous and has a chemical composition typical of volcanic-arc tectonic setting. Late- to post-tectonic granites are described in the Dronning Maud Land, Antarctica. The Dalmantian Granite (Grantham *et al.*, 1991) is one of the best known. However, the chemistry and genesis of this granite as described by Grantham *et al.* (1991) differs from the Tchinhadzandze Granodiorite Gneiss in that the former is a typical S-type granite with SiO_2 contents of ~73-~75 wt%, is biotite-muscovite bearing, forms sheet-like sills commonly parallel to layering and has Rb, Nb and Y contents typical of syn-collisional granites.

13.2 Deformation

The planar structures in the Archaean granite-greenstone belt are dominantly oriented E-W whereas in the Mozambique Metamorphic Province are E-W and N-S.

In the greenstones two deformation episodes are recognized, namely D_1 associated with the development of an S_1 foliation parallel to the S_0 primary layering, and D_2 which folds these fabrics about axes which plunge shallowly to the east implying a N-S compression. Towards the E, in the Messica-Garuzo area, the D_1 episode gave rise to S_1 planar fabrics which are sub-parallel to S_0 primary layering preserved in the metasediments of the Frontier Formation.

Within the Mozambique Metamorphic Province the structures are more complex. Thus, in the Vanduzi Migmatite Gneiss two deformation events are preserved. D_1 produced a more or less E-W striking S_1 planar fabric parallel to S_0 primary layering and the development of leucosomes with similar orientation to the foliation. D_2 deformed the S_0 and S_1 planar fabrics about more or less N-S axes resulting in the development of N-S planar fabrics which include the S_2 foliation and second stage leucosomes. Farther east, within the megacrystic Nhansipfe Granitic Orthogneiss both planar and linear structures have highly variable orientations which possibly record complex deformation processes. In the Chimoio Granodioritic Gneiss the planar fabrics strike N-S and linear fabrics suggest the development of zones of shallow and steep fabrics possibly as a result of oblique strike-slip movement imposed on an earlier shallow dipping fabric. The Tchinhadzandze Granodiorite Gneiss have weak , variable planar and linear fabrics consistent with its syn-to post-tectonic granite nature.

13.3 Metamorphism

The metamorphism in the greenstone reached the low -grade greenschist facies and P-T conditions are constrained at 400-500 °C and <4 kbar. In the granites a later heating is recorded by biotite resetting at ~1100 Ma (Fig. 13.2) and was, possibly, caused by intrusions of granitoids in the Mozambique Metamorphic Province or by Umkondo related mafic intrusions.

The Frontier Formation is characterized by two different metamorphic grades. The block around Garuzo is defined by a paragenesis including Sil+Grt whereas in the block in Chimezi the paragenesis include the higher pressure assemblage Sil+Ky . The medium -grade high pressures assemblage of Sil+Ky in the Chimezi area can be considered anomalous because the Frontier Formation rocks overlie the Manica Greenstone Belt rocks which have a relatively low pressure andalusite-bearing low-grade assemblages. The assemblage Sil+Grt+Bt in the presence of Qtz and Ms in the pelitic schists suggests metamorphic constraints of T=~680 °C and P=~8 kbar typical of medium- to high-grade metamorphism (Winkler, 1974, p. 216). The Early Proterozoic Messica Granite Gneiss, which underlies the Frontier Formation does not record obvious metamorphic mineral growth. This anomaly may, therefore, suggest that the Frontier Formation has been overthrust onto the Archaean granite-greenstone belt and would support the possible allochthonous nature of the unit.

Within the Mozambique Metamorphic Province the metamorphism reached medium- to high-grades whereby higher degrees are registered farther east. P-T conditions are constrained at ~530-~980 °C and
~5-~10 kbar. There is evidence of later thermal processes as is suggested by mineral resetting. The Messica Granite Gneiss and the Chimoio Granodioritric Gneiss record biotite resetting at ~550 Ma significantly different, in terms of geological time, to ~460 Ma recorded by biotite and muscovite resetting in the Nhansipfe Granitic Orthogneisses and the Garuzo Frontier Formation quartzite. This mineral resetting took place in localized zones coinciding with the Messica Granite Gneiss, Vanduzi Migmatitic Gneiss and Nhansipfe Granitic Orthogneiss where strong N-S partial melt bands occurred, suggesting that the partial melts may be a result of same process that caused the mineral resetting.

In conclusion, there is an increase of metamorphic grade from low greenschist facies within the

greenstone belt in the W to medium - to high-grade amphibolitic facies within the Mozambique Metamorphic Province in the E. This, combined with the structural data, can be summarized in Figure 13.1. The figure suggests that the blocks of low (LG), medium (MG) and high (HG) grades are separated from each other by N-S steep zones. The lineations in these steep zones commonly plunge shallowly suggesting that they represent oblique shear zones with combined lateral and vertical displacements.

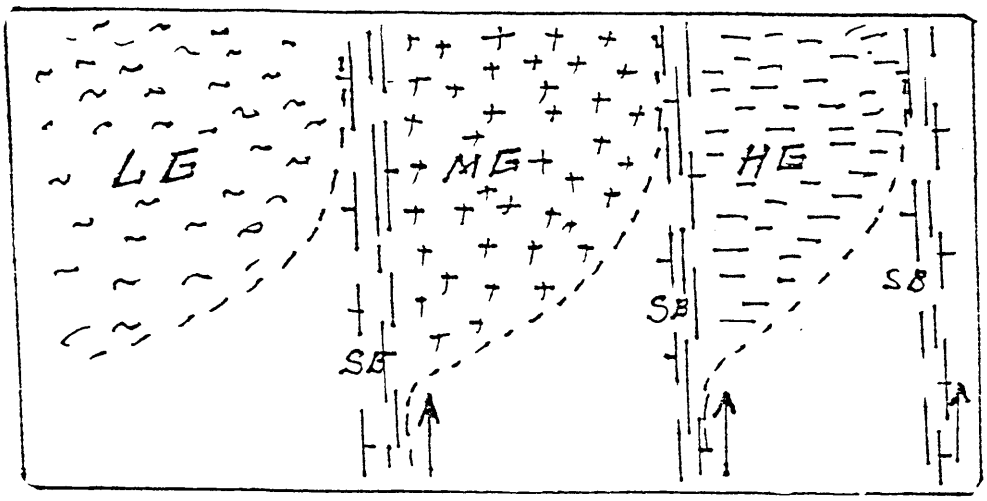

Figure 13.1: Sketch of metamorphic blocks separated by steep zones defining narrow shear belts (SB). LG- block of low grade, MG- block of medium grade and HG- block of high grade. Arrows indicate lateral movement.

Similar deformational and metamorphic conditions as described for the Mozambique belt are observed in Antarctica (Grantham *et al.*, 1988; Grantham *et al.*, 1991; Groenwald *et al.*, 1991; Groenwald, 1993; Grantham *et al.*, 1994; Grantham *et al.*, 1995 and Grantham *et al.*, 1997).

13.4 Isotope Chemistry

The chronological aspects of radiogenic isotope analyses have been discussed in the relevant chapters. This section will consider the implications for the sources of the various granitoids arising from the isotope analyses.

The initial $^{87}Sr/^{86}Sr$ ratios data including those of Manuel (1992) are plotted versus age in the diagram of Figure 13.2. The diagram includes a curve showing the evolution of initial $^{87}Sr/^{86}Sr$ ratios with time in the mantle. The crosses are proportional to the error of either Ro and ages. It can be seen that both the old granites and the Chimoio gneisses have initial $^{87}Sr/^{86}Sr$ ratios close to that of the mantle suggesting their derivation from it. Conversely, the initial $^{87}Sr/^{86}Sr$ ratios of the remaining units are high above the mantle growth curve which suggest that their sources probably had a significant component of older continental crust.

The R_o of ~0.6947 in the ~3400 Ma in the northern Vumba Granitic Gneiss is compatible with the derivation of this gneiss from the mantle (Rollinson, 1993).

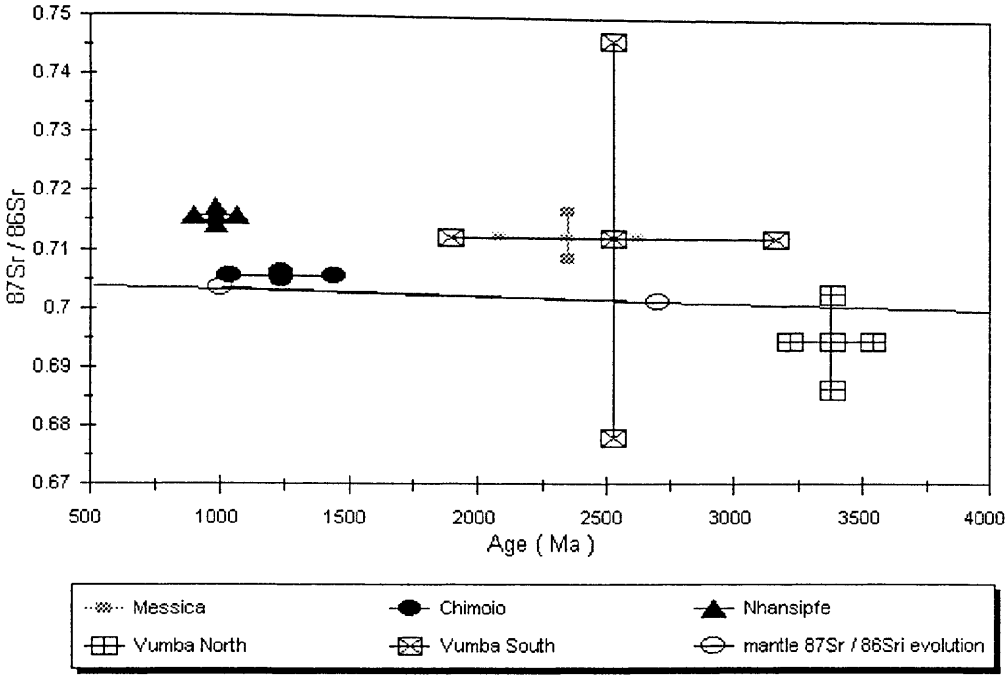

Figure 13.2: Initial $^{87}Sr/^{86}Sr$ ratios versus age of some lithological units. The mantle initial $^{87}Sr/^{86}Sr$ ratios evolution curve is drawn, modified from Rollinson (1993).

The ~2900 Ma non-foliated granite has a R_0 of ~0.7052 (Manuel, 1992) which is very high for the determined age, falling within the limits of subduction related arc-volcanics of 0.7033-0.7095 (Rollinson, 1993), and implies that the magma has been produced from an enriched source. Indistinguishable initial $^{87}Sr/^{86}Sr$ ratios of ~0.7122 and ~0.71241 from the ~2527 Ma granite south of the greenstone (Manuel, 1992) and the ~2347 Ma Messica Granite Gneiss respectively are very high and clearly suggest that their source had high Sr/Rb ratios.

The R_0 of ~0.7056 in the ~1236 Ma Chimoio Granodiorite Gneiss falls within the limits of the arc-volcanic ratios of 0.7033 -0.7095 (Rollinson, 1993) and is consistent with its subduction related arc-volcanic genesis as suggested from geochemistry. The Ro is only marginally higher than the mantle growth curve at the that time suggesting that the Chimoio Granodioritic Gneiss is relatively juvenile.

The R_0 of 0.7157 of Nhansipfe Granitic Othogneiss is compatible with the magma source from an already enriched crust which is consistent with the plate margins of a within-plate tectonic environment of formation of this granite.

13.5 Summary of the Geology of The Study Area and a Comparison with Antarctica

The summary and comparison of the geology are given in Table 13.1 and the temperature-time conditions are shown in Figures 13.3 and 13.4. The table shows that the geology of the study area is so similar to that of Antarctica and that correlations between the two areas are possible. Similarly, for the equivalent period of time, comparison of temperature-time diagrams of the two regions (Fgs. 13.3 and 13.4) show that they experienced similar thermal conditions.

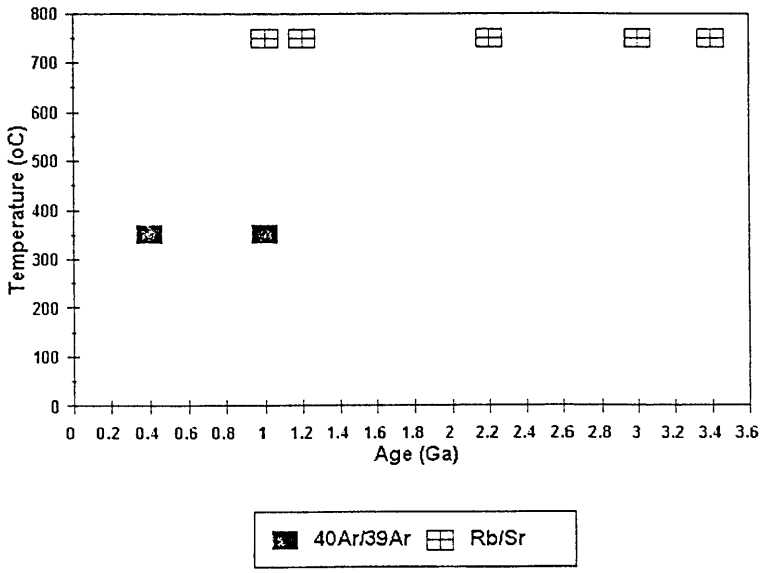

Figure 13.3: Temperature-time diagram for the mineralogical Ar/Ar and whole rock Rb/Sr data determined from the granites and the metasediments in Manica.

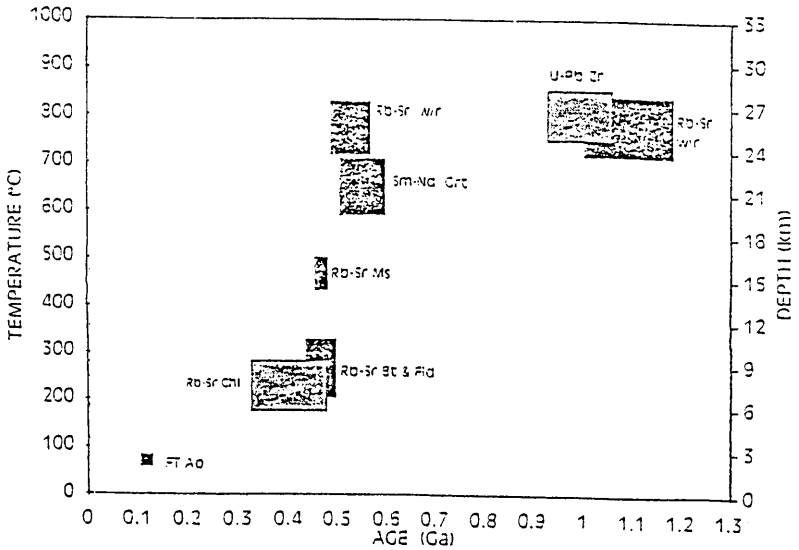

Figure 13.4: Temperature-time diagram for the various mineralogical and whole rock data determined from H.U. Sverdrupfjella. Grt- garnet, Bt- biotite, Chl- chlorite, Ms- muscovite, Zr- zircon and Fld- feldspar; W/r- whole rock; FT- fission track. Diagram reproduced from Grantham *et al.* (1995).

Table 13.1: Summary and comparison of the geologies of study area and Antarctica.

Lithology	Mozambique	Antarctica
	Vumba Granite Gneiss medium to coarse-grained metaluminous Hbl and Bt granodiorite to tonalite gneiss **Manica Greenstones** serpentinites, mafic to ultramafic schist, pelitic schist and felsic schist. **Chimoio Granodiorite Gneiss** medium -grained metaluminous Bt-Hbl quartz feldspathic gneiss **Nhansipfe Granitic Orthogneiss** megacrystic metaluminous to peraluminous Bt+Grt±Hbl quartzo-feldspathic augen gneiss **Mafic Intrusions** N-S oriented medium grained Plg+Hbl+Grt±Cpx±Opx amphibolitic dykes **Syn-to Post Tectonic Intrusions** Thcinhadzandze Granodiorite Gneiss	**Annandagstoppane Granite** medium - to coarse-grained peraluminous Bt tonalitic to granodioritic gneiss (Barton *et al.* 1987). No equivalent exposed **Jutulrora Formation** Ep-Bt-Hbl tonalitic quartz feldspar gneisses (Grantham *et al.*, 1988; Grantham *et al.*, 1995; Grantham *et al.*, 1997) **Kirwanveggen Megacrystic Orthogneiss** Bt±Grt±Hbl quartzo-feldspathic augen gneiss (Grantham *et al*, 1988; Grantham *et al.*, 1995) **Mafic Intrusions** Plg+Hbl+Grt±Cpx±Opx metabasites (Grantham *et al.*, 1988) **Syn-Tectonic Intrusions** Dalmatian Granite (Grantham *et al.*, 1991)

Structural Geology	**In the Archaean Zimbabwe Craton** Early deformation associated with metamorphism in the old granites resulting in their transformation into gneisses. Deformation associated with the greenschist metamorphism which resulted in the N and S moderately dipping, S_1 planar fabrics Deformation associated with the folding of S_1 along an E-W axis **In the Proterozoic Mozambique Metamorphic Province** Deformation associated with E and W moderately and steeply dipping S_1 planar fabrics Deformation associated with the amphibolitic facies metamorphism which resulted in the E and W steeply dipping S_2 planar fabrics which were transposed onto S_1 Deformation associated with the N-S shear zones and linear fabrics trending N and S mostly with shallow to moderate angles	**In the Archaean** Early deformation associated with metamorphism in the old granites resulting in their transformation into gneisses (Barton *et al.*, 1987) no equivalent recognized **In the Proterozoic** Deformation associated with S_1 N-S trending and gently dipping to both east and west planar fabrics Deformation associated with shear zones and folds which deform S_1, shallowly plunging mineral lineation towards 110° and 290°, in Haag Nunataks (Grantham *et al.*, 1997) Deformation associated with the south, mostly, dipping planar fabrics, shallowly plunging lineations towards 110°, in Western Sverdrupfjella (Grantham *et al.*,1988; Grantham *et al.*, 1995) Deformation associated with the southeast east and west dipping planar fabrics Lineations plunging shallowly towards 120° and 130° in Kirwanveggen (G* *et al*, 1988; G* *et al.*, 1991; Grantham *et al.*,1995)

Metamorphic History	**In the Archaean Zimbabwe Craton** Medium grade and retrogressive hydration reactions in the Vumba Granite Gneisses Mineral (biotite) resetting at ~1.1 Ga (Fig. 13.3) Greenschist facies metamorphism in the greenstones **In the Proterozoic Mozambique Metamorphic Province** Medium grade amphibolite facies Mineral (biotite and muscovite) resetting suggest heating at ~470 Ma and ~550 Ma (Fig. 13.3)	**In the Archaean** Medium grade and retrogressive hydration reactions in the Annandagstoppane Granite Gneisses (Barton *et al.*, 1987) mineral resetting at ~1.1-~1.2 Ga (Fig. 13.4) no equivalent recognized **In the Proterozoic** Medium grade amphibolite facies mineral resetting In H.U. Sverdrupfjella data indicate mineral setting at ~450 Ma (Fig. 13.4) (Grantham *et al.*, 1988 ; Grantham *et al.* 1994; Grantham *et al.* (1995)

G*=Grantham.

13.6 Proposed Geological Evolution Model for the Study Area

These data suggest that the geological evolution of the study area comprises:

1- The Emplacement of the Vumba old granitoids (~3300 -~3000 Ma) as mantle derivatives and the consequent formation of an old granitic basement

2- The emplacement of the ophiolitic komatiites from mantle peridotites

4- Deposition of pelitic sediments in a deep still water environment

5- ---------- **Metamorphism (M_1) / Deformation (D_1/D_2)** ----------

Low grade metamorphism to greenschist facies of the komatiites and sediments

retrogressive dehydration reactions in the granitoids

development of schistosity in the komatiites and sediments (D_1)

folding of planar fabrics in the pelitic schist (D_2)

6- Emplacement of Messica Granite Gneiss and Vumba younger granitoids (~2650 -~2350 Ma) from partial melting of the already formed granitic crust

7- ---------- **Cratonization** ----------

Formation of the Zimbabwe Craton

8- Emplacement of the possible allochthonous Frontier Formation

9- ---------- **Subduction related processes / Mozambique Orogeny** ----------

Formation of an island-arc to the east of Zimbabwe Craton (eg. Pinna *et al.* 1993)

Collision of Zimbabwe Craton (ZC) with the island arc which resulted in:

Accretion of the island onto the craton to form the Chimoio Granodiorite Gneiss (~1200 Ma)

Emplacement of the Nhansipfe Granitic Orthogneiss (~1000 Ma)

Metamorphism (M_1)/Deformation (D_1/D_2)

- medium to high grade amphibolite to granulite facies metamorphism (M_1)
- migmatization (Vanduzi Migmatitic Gneiss)
- development of S_1 E-W planar fabrics (D_1)
- development of S_2 N-S planar fabrics (D_2)

9- Intrusion of mafic dykes in an extensional/rifting environment

10- ---------- **Pan-African Orogeny** ----------

Metamorphism (M_2)

- medium to high grade metamorphism and development of second stage leucosomes in the Vanduzi Migmatitic Gneiss

-Syn- to post-tectonic emplacement of Tchinhadzandze Granodiorite Gneiss